APPLICATION OF FRACTURE MECHANICS IN ASSESSMENT OF STRUCTURAL INTEGRITY

Prof. dr Aleksandar Sedmak,

Faculty of Mechanical Engineering, University of Belgrade, Serbia

- Linear Elastic Fracture Mechanics, stress intensity factor, fracture toughness
- Plastic zones, a step toward Elastic-Plastic Fracture Mechanics
- Structural integrity – Assessment by using fracture mechanics parameters
- Example of structural integrity assessment
- Testing of AMM, K_{Ic} measurement
- Fatigue, Paris law, (remaining) life, da/dN vs. a
- Example of static and dynamic crack growth analysis – hip implant
- Conclusions

Stress concentration

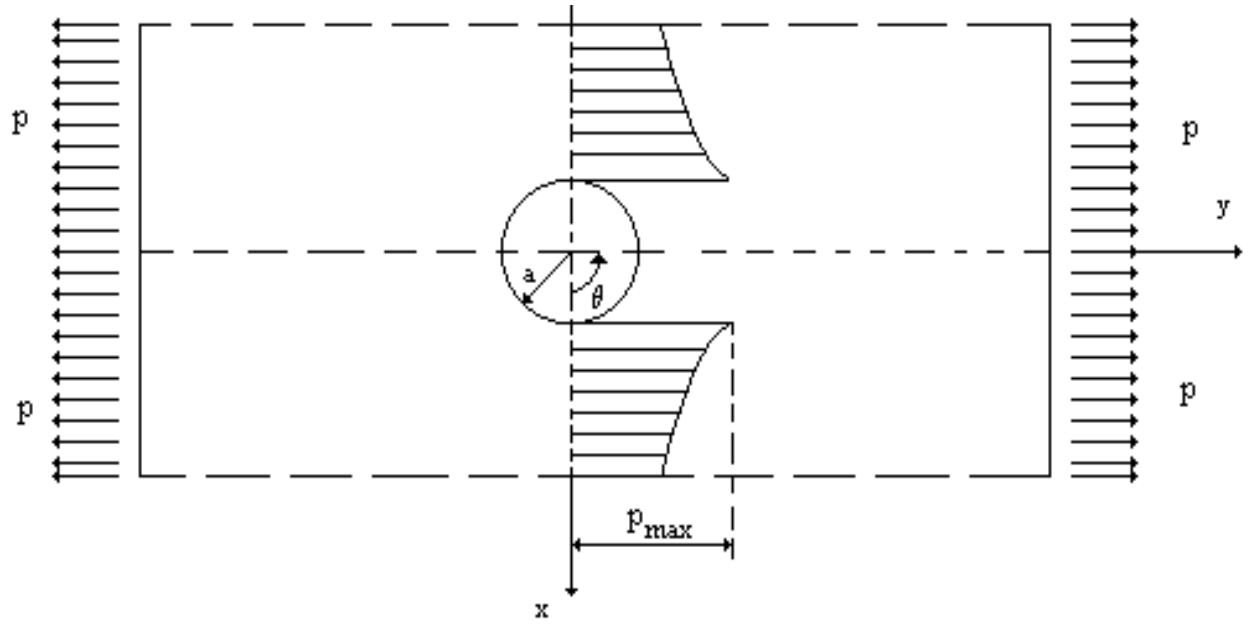

p_{max}=3p, three times the value of average stress p in cross section of circular hole.

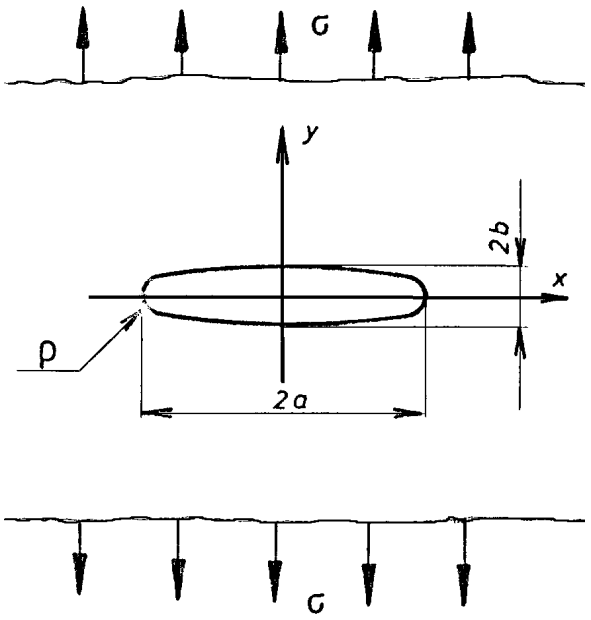

Let us consider the case of **elliptic hole in an infinite plate, the max. stress is:**

$$\sigma_{max} = \sigma\left(1+\frac{2a}{b}\right) = \sigma\left[1+2\left(\frac{a}{\rho}\right)^{1/2}\right]$$

where a stands for ellipse major axis, b for minor axis, σ is normal stress in remote section, ρ ellipse root radius ($\rho=b^2/a$). If minor axis $b \to 0$ (or, this is the same $\rho \to 0$) normal stress will tend to infinity ($\sigma_{yy} \propto$), and in elastically deformed material the condition for fracture is fulfilled, e.g. the component will be broken in brittle manner just after load is applied. So, we can't do much about cracks with this classic stress analysis. Simply, stress concentration doesn't work.

Linear Elastic Fracture Mechanics

The Elastic Stress Field Approach

The Stress Intensity Factor

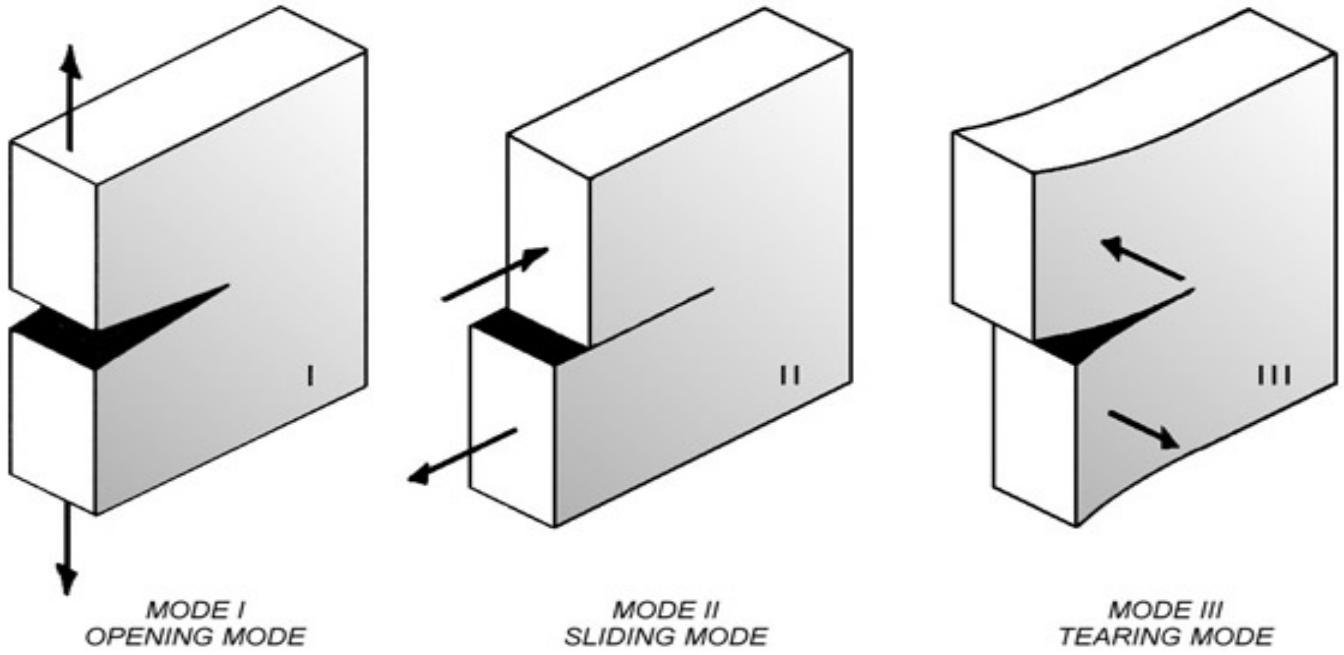

The three basic modes of crack surface displacements

Derivation of the Elastic Stress Field Equations

- Concepts of plane stress and plane strain
- Equilibrium equations
- Compatibility equations for strains
- Airy stress function
- Biharmonic equation
- Complex stress functions: **Westergaard function for biaxially loaded plate (Mode I)**
- Mode I stress / displacement fields
- Mode I stress intensity factor

Westergard (1939), Irwin (1957)

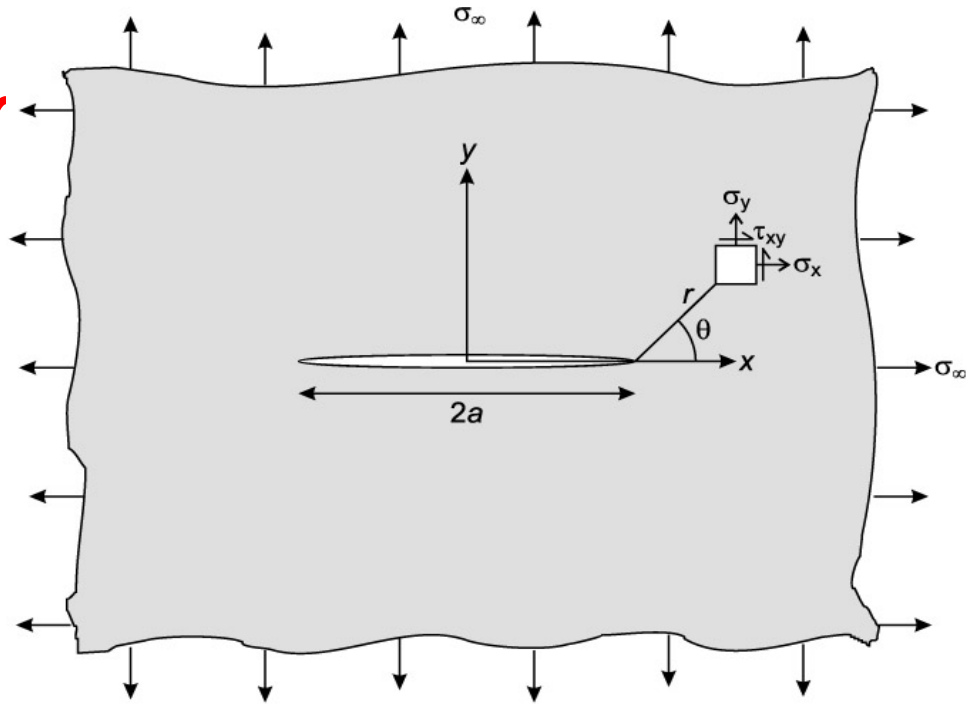

$$\sigma_X = \frac{\sigma\sqrt{\pi a}}{\sqrt{2\pi r}}\cos\frac{\theta}{2}\left(1-\sin\frac{\theta}{2}\sin\frac{3\theta}{2}\right)$$

$$\sigma_Y = \frac{\sigma\sqrt{\pi a}}{\sqrt{2\pi r}}\cos\frac{\theta}{2}\left(1+\sin\frac{\theta}{2}\sin\frac{3\theta}{2}\right)$$

$$\tau_{XY} = \frac{\sigma\sqrt{\pi a}}{\sqrt{2\pi r}}\sin\frac{\theta}{2}\cos\frac{\theta}{2}\cos\frac{3\theta}{2}$$

Linear Elastic Crack-tip Fields

(general case)

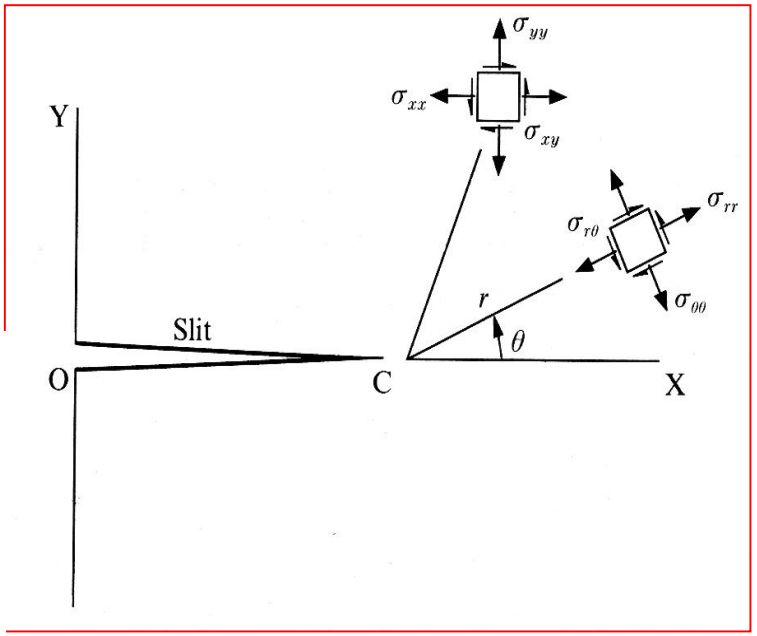

Mode I:

$$\kappa = (3-\nu)/(1+\nu), \quad \nu' = 0, \quad \nu'' = \nu, \quad \text{(plane stress)}$$
$$\kappa = (3-4\nu), \quad \nu' = \nu, \quad \nu'' = 0, \quad \text{(plane strain)}.$$

$$\begin{Bmatrix}\sigma_{xx}\\ \sigma_{yy}\\ \sigma_{xy}\end{Bmatrix} = \frac{K_I}{(2\pi r)^{1/2}} \begin{Bmatrix}\cos(\theta/2)\,[1-\sin(\theta/2)\sin(3\theta/2)]\\ \cos(\theta/2)\,[1+\sin(\theta/2)\sin(3\theta/2)]\\ \sin(\theta/2)\cos(\theta/2)\cos(3\theta/2)\end{Bmatrix}$$

$$\begin{Bmatrix}\sigma_{rr}\\ \sigma_{\theta\theta}\\ \sigma_{r\theta}\end{Bmatrix} = \frac{K_I}{(2\pi r)^{1/2}} \begin{Bmatrix}\cos(\theta/2)\,[1+\sin^2(\theta/2)]\\ \cos^3(\theta/2)\\ \sin(\theta/2)\cos^2(\theta/2)\end{Bmatrix}$$

$$\sigma_{zz} = \nu'(\sigma_{xx}+\sigma_{yy}) = \nu'(\sigma_{rr}+\sigma_{\theta\theta})$$

$$\sigma_{xz} = \sigma_{yz} = \sigma_{rz} = \sigma_{\theta z} = 0$$

$$\begin{Bmatrix}u_x\\ u_y\end{Bmatrix} = \frac{K_I}{2E}\left\{\frac{r}{2\pi}\right\}^{1/2} \begin{Bmatrix}(1+\nu)\,[(2\kappa-1)\cos(\theta/2)-\cos(3\theta/2)]\\ (1+\nu)\,[(2\kappa+1)\sin(\theta/2)-\sin(3\theta/2)]\end{Bmatrix}$$

$$\begin{Bmatrix}u_r\\ u_\theta\end{Bmatrix} = \frac{K_I}{2E}\left\{\frac{r}{2\pi}\right\}^{1/2} \begin{Bmatrix}(1+\nu)\,[(2\kappa-1)\cos(\theta/2)-\cos(3\theta/2)]\\ (1+\nu)\,[-(2\kappa+1)\sin(\theta/2)+\sin(3\theta/2)]\end{Bmatrix}$$

$$u_z = -(\nu'' z/E)(\sigma_{xx}+\sigma_{yy}) = -(\nu'' z/E)(\sigma_{rr}+\sigma_{\theta\theta}).$$

Mode II:

$$\begin{Bmatrix}\sigma_{xx}\\ \sigma_{yy}\\ \sigma_{xy}\end{Bmatrix} = \frac{K_{II}}{(2\pi r)^{1/2}}\begin{Bmatrix}-\sin(\theta/2)\,[2+\cos(\theta/2)\cos(3\theta/2)]\\ \sin(\theta/2)\cos(\theta/2)\cos(3\theta/2)\\ \cos(\theta/2)\,[1-\sin(\theta/2)\sin(3\theta/2)]\end{Bmatrix}$$

$$\begin{Bmatrix}\sigma_{rr}\\ \sigma_{\theta\theta}\\ \sigma_{r\theta}\end{Bmatrix} = \frac{K_{II}}{(2\pi r)^{1/2}}\begin{Bmatrix}\sin(\theta/2)\,[1-3\sin^2(\theta/2)]\\ -3\sin(\theta/2)\cos^2(\theta/2)\\ \cos(\theta/2)\,[1-3\sin^2(\theta/2)]\end{Bmatrix}$$

$$\sigma_{zz} = \nu'(\sigma_{xx}+\sigma_{yy}) = \nu'(\sigma_{rr}+\sigma_{\theta\theta})$$

$$\sigma_{xz} = \sigma_{yz} = \sigma_{rz} = \sigma_{\theta z} = 0$$

$$\begin{Bmatrix}u_x\\ u_y\end{Bmatrix} = \frac{K_{II}}{2E}\left\{\frac{r}{2\pi}\right\}^{1/2}\begin{Bmatrix}(1+\nu)\,[(2\kappa+3)\sin(\theta/2)+\sin(3\theta/2)]\\ -(1+\nu)\,[(2\kappa-3)\cos(\theta/2)+\cos(3\theta/2)]\end{Bmatrix}$$

$$\begin{Bmatrix}u_r\\ u_\theta\end{Bmatrix} = \frac{K_{II}}{2E}\left\{\frac{r}{2\pi}\right\}^{1/2}\begin{Bmatrix}(1+\nu)\,[-(2\kappa-1)\sin(\theta/2)+3\sin(3\theta/2)]\\ (1+\nu)\,[-(2\kappa+1)\cos(\theta/2)+3\cos(3\theta/2)]\end{Bmatrix}$$

$$u_z = -(\nu'' z/E)\,(\sigma_{xx}+\sigma_{yy}) = -(\nu'' z/E)\,(\sigma_{rr}+\sigma_{\theta\theta}).$$

Mode III:

$$\sigma_{xx} = \sigma_{yy} = \sigma_{rr} = \sigma_{\theta\theta} = \sigma_{zz} = 0$$

$$\sigma_{xy} = \sigma_{r\theta} = 0$$

$$\begin{Bmatrix}\sigma_{xz}\\ \sigma_{yz}\end{Bmatrix} = \frac{K_{III}}{(2\pi r)^{1/2}}\begin{Bmatrix}-\sin(\theta/2)\\ \cos(\theta/2)\end{Bmatrix}$$

$$\begin{Bmatrix}\sigma_{rz}\\ \sigma_{\theta z}\end{Bmatrix} = \frac{K_{III}}{(2\pi r)^{1/2}}\begin{Bmatrix}\sin(\theta/2)\\ \cos(\theta/2)\end{Bmatrix}$$

$$u_x = u_y = u_r = u_\theta = 0$$

$$u_z = (4K_{III}/E)\,(r/2\pi)^{1/2}\,[(1+\nu)\sin(\theta/2)].$$

CHARACTERISTICS OF THE STRESS FIELDS

- The stress and displacement formulas may reduced to particularly simple forms:

$$\sigma_{ij} = K(2\pi r)^{-1/2} f_{ij}(\theta)$$

$$u_i = (K/2E)\,(r/2\pi)^{1/2} f_i(\theta)$$

Applied loading enters ***only through K*** !!

for the infinite plate: $K = \sigma(\pi * a)^{1/2}$

but for a given Mode **there is a characteristic *shape* of the field** !!!

Principle of Superposition: for a given Mode, K terms from superposed loadings are additive

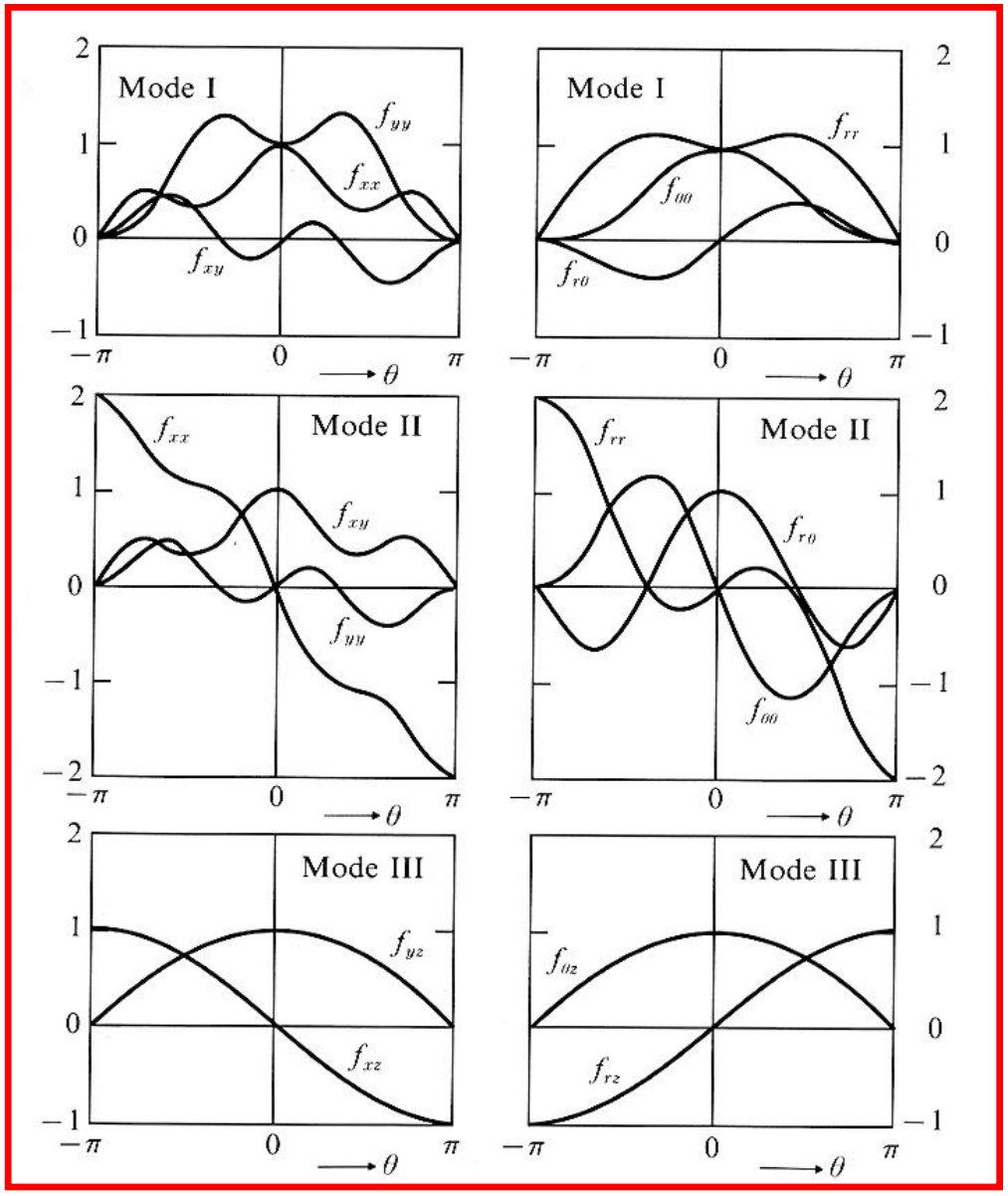

Angular distributions of crack-tip stresses for the three modes (rectangular: left; polar:right)

We consider next some other cases apart from the cracked infinite plate

- Semi infinite edge notched specimens
- Finite width centre cracked specimens
- Finite width edge notched specimens

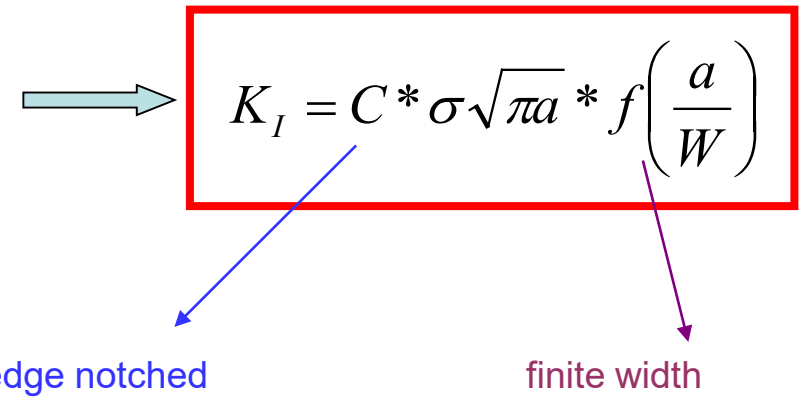

-Crack-line loading

-Elliptical / Semielliptical cracks

Finite-width centre-craked specimens:

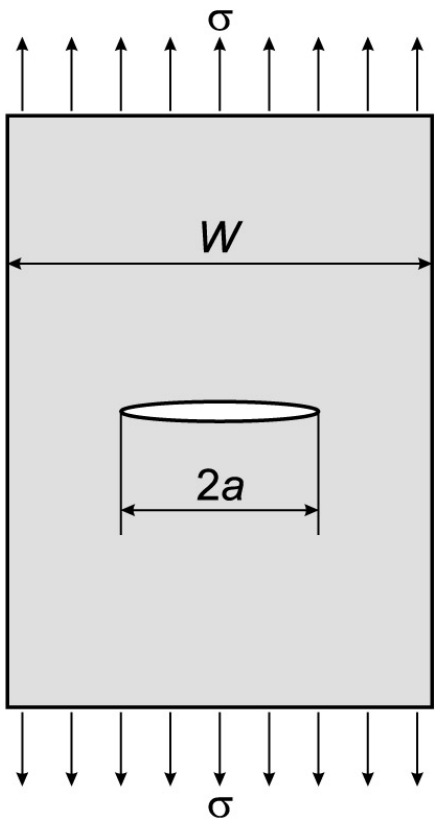

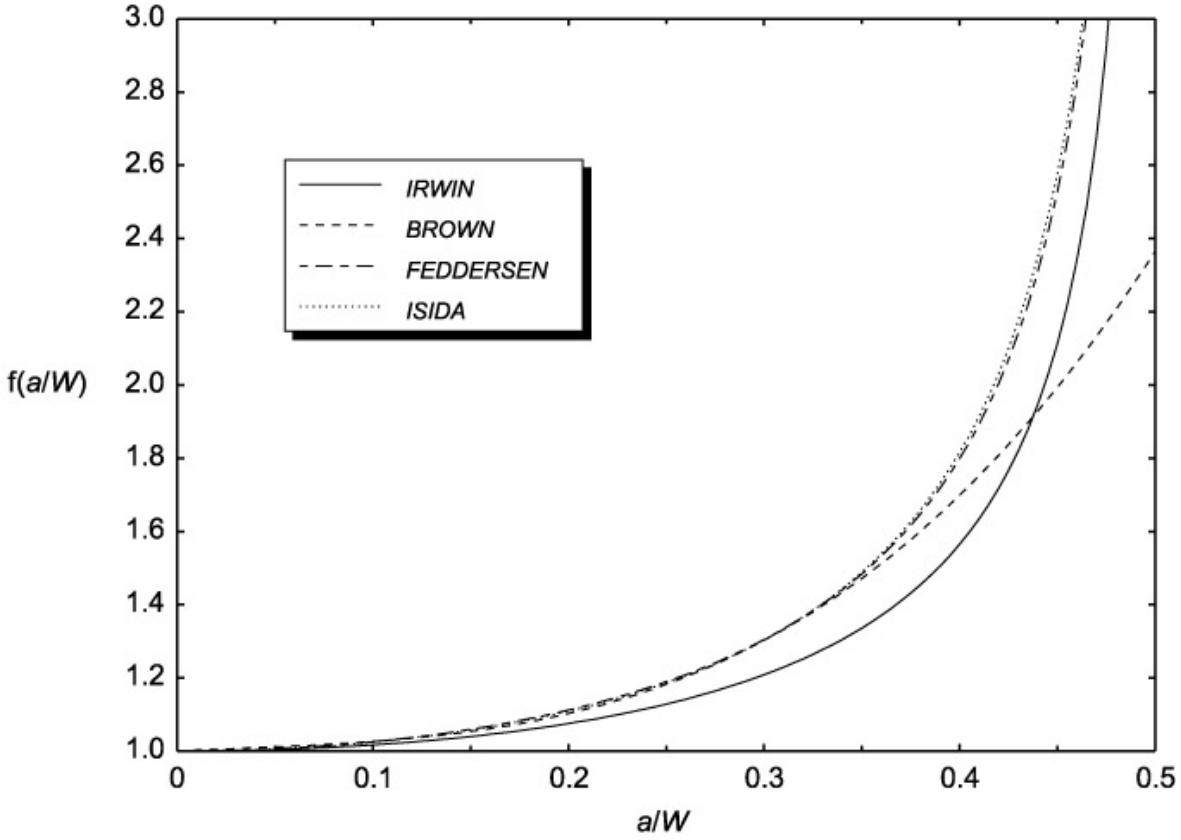

f(a/W)

Irwin: $K_I = \sigma\sqrt{\pi a}\sqrt{\frac{W}{\pi a}\tan\left(\frac{\pi a}{W}\right)}$

Isida: 36 term power series

approx. →

Brown: $f\left(\frac{a}{W}\right) = 1 + 0.256\left(\frac{a}{W}\right) - 1.152\left(\frac{a}{W}\right)^2 + 12.200\left(\frac{a}{W}\right)^3$

Feddersen: $K_I = \sigma\sqrt{\pi a}\sqrt{\sec\left(\frac{\pi a}{W}\right)}$

Semi infinite edge-notched specimens:

Free edges: crack opens more than in the infinite plate resulting in 12% increase in stress, not to mention crack size!

$$K_I = 1.12 * \sigma\sqrt{\pi a}$$

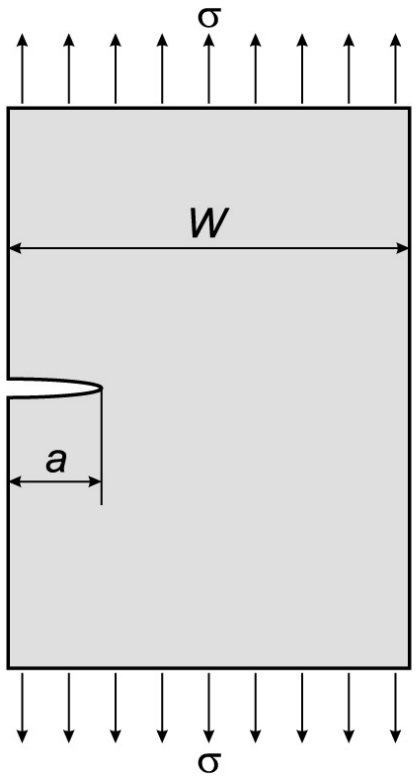

Single edge notched (SEN)

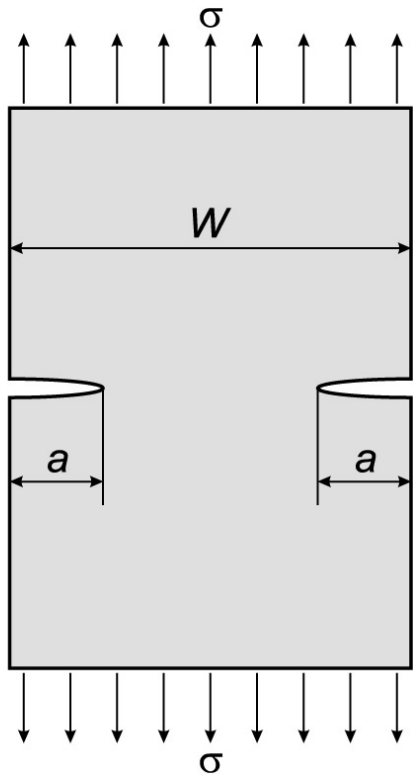

Double edge notched (DEN)

Finite-width edge-notched specimens:

SEN: $$K_I = \sigma\sqrt{\pi a} * \left(1.122 - 0.231\left(\frac{a}{W}\right) + 10.550\left(\frac{a}{W}\right)^2 - 21.710\left(\frac{a}{W}\right)^3 + 30.382\left(\frac{a}{W}\right)^4\right)$$

0.5% accurate for a/W < 0.6

DEN: $$K_I = \sigma\sqrt{\pi a} * \frac{1.122 - 1.122\left(\frac{a}{W}\right) - 0.820\left(\frac{a}{W}\right)^2 + 3.768\left(\frac{a}{W}\right)^3 - 3.040\left(\frac{a}{W}\right)^4}{\sqrt{1 - \frac{2a}{W}}}$$

0.5% accurate for any a/W

TWO IMPORTANT SOLUTIONS FOR PRACTICAL USE

* Crack-line Loading

(P: force per unit thickness)

$$K_{IA} = \frac{P}{\sqrt{\pi a}}\sqrt{\frac{a+x}{a-x}}$$

$$K_{IB} = \frac{P}{\sqrt{\pi a}}\sqrt{\frac{a-x}{a+x}}$$

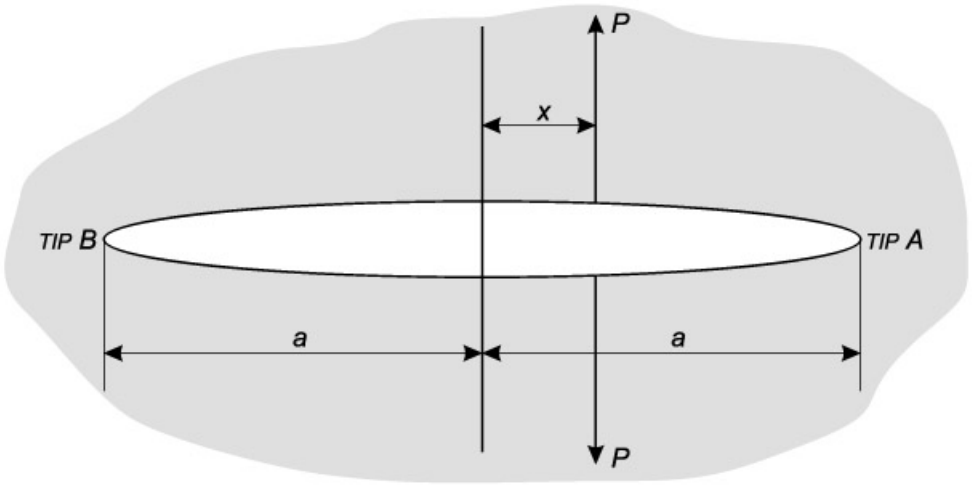

for centrally located force:

$$K_I = \frac{P}{\sqrt{\pi a}}$$

K_I decrease when crack length increases !

Very useful solution:

- Riveted, bolted plates
- Internal Pressure problems →

Crack under internal pressure (force per unit thickness is now P.dx, where P is the internal pressure)

$$K_I = \frac{P}{\sqrt{\pi a}}\int_{-a}^{a}\sqrt{\frac{a-x}{a+x}}\,dx = \frac{P}{\sqrt{\pi a}}\int_{0}^{a}\left(\sqrt{\frac{a+x}{a-x}}+\sqrt{\frac{a-x}{a+x}}\right)dx$$

$$K_I = \frac{P}{\sqrt{\pi a}}\int_{0}^{a}\frac{2a}{\sqrt{a^2-x^2}}dx = \frac{2Pa}{\sqrt{\pi a}}\left[\arcsin\frac{x}{a}\right]_0^a = P\sqrt{\pi a}$$

same result by end loading with σ !

* Elliptical Cracks

actual cracks often initiate at surface discontinuities or corners in structural components !!!

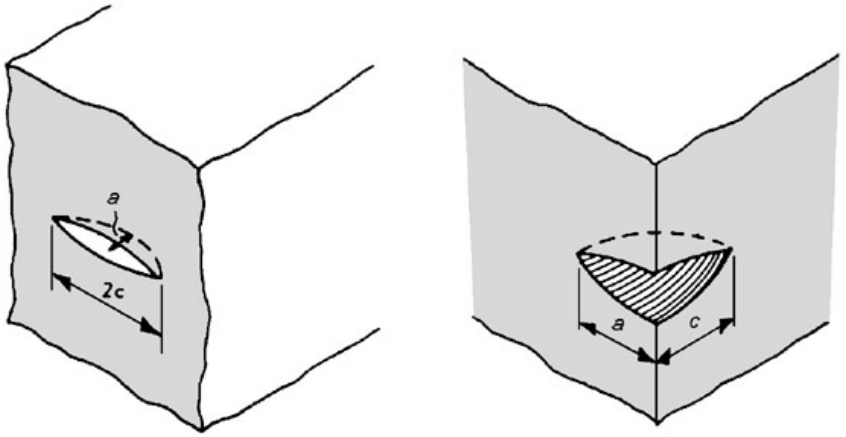

We start considering idealised situations:

from embeded elliptical crack to

Semi-elliptical surface cracks

Example: corner crack in a longitudinal section of a pipe-vessel intersection in a pressure vessel

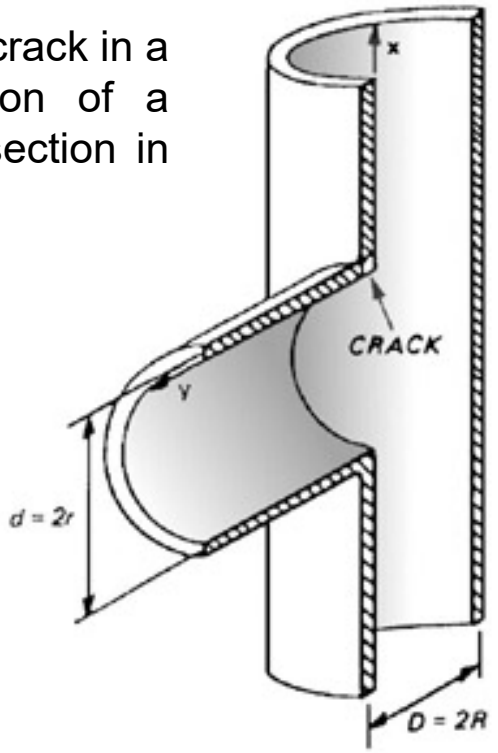

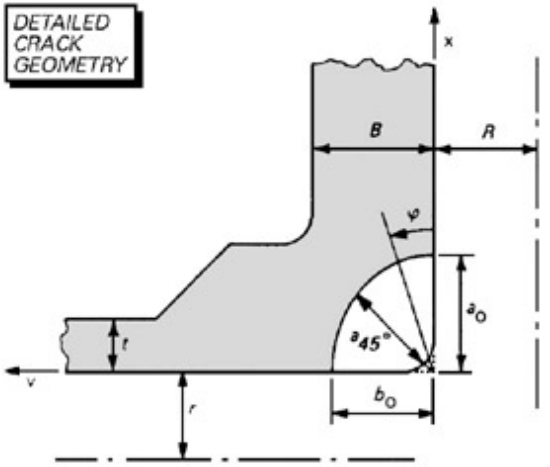

The embeded (infinite plate) elliptical crack under Mode I loading

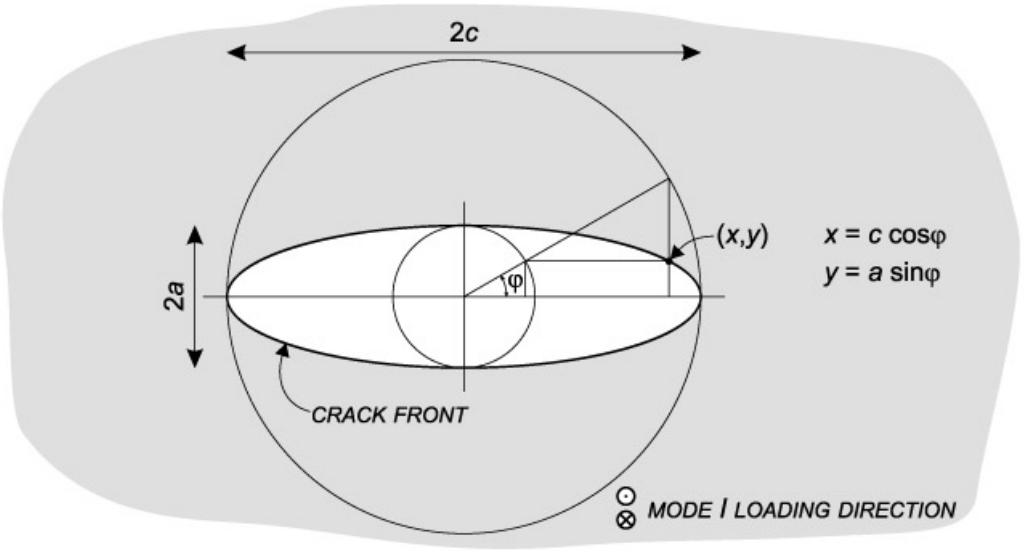

Irwin solution for Mode I:

$$K_I = \frac{\sigma\sqrt{\pi a}}{\Phi}\left(\sin^2\varphi + \frac{a^2}{c^2}\cos^2\varphi\right)^{1/4}$$

Where Φ: elliptic integral of the second type

$$\Phi = \int_0^{\pi/2} \sqrt{1-\sin^2\alpha\sin^2\varphi}\, d\varphi$$

with: $\sin^2\alpha = \frac{\left(c^2 - a^2\right)}{c^2}$

a/c	0.0	0.1	0.2	0.3	0.4	0.5	0.6	0.7	0.8	0.9	1.0
Φ	1.000	1.016	1.051	1.097	1.151	1.211	1.277	1.345	1.418	1.493	1.571

circular crack:

$$K_I = \frac{2}{\pi} * \sigma\sqrt{\pi a}$$

K_I varies along the elliptical crack front

max. at $\varphi = \pi/2$:

$$K_I = \frac{1}{\Phi} * \sigma\sqrt{\pi a}$$

min. at $\varphi = 0$:

$$K_I = \frac{\sigma\sqrt{\pi\left(a^2/c\right)}}{\Phi}$$

During crack growth an elliptical crack will tend to become circular: important in fatigue problems

The semi- elliptical surface crack in a plate of finite dimensions under Mode I loading

In practice elliptical cracks will generally occur as semi-elliptical surface cracks or quarter-elliptical corner cracks. Best solutions for semi-elliptical: FEM calculations from Raju-Newman:

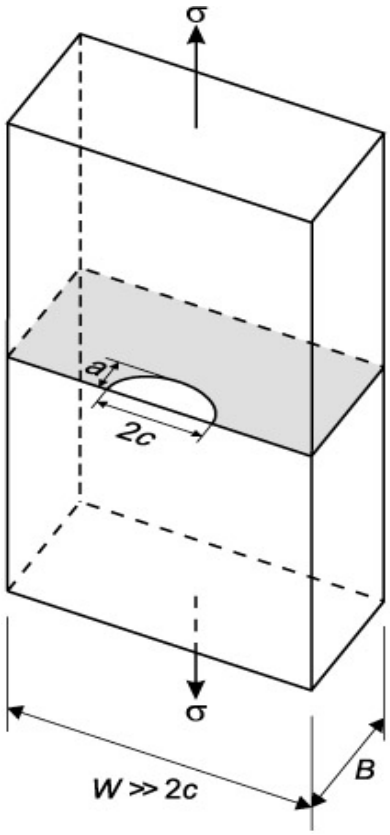

$K = C\sigma\sqrt{\pi a}/\phi$

a/c	φ	C, a/B = 0.2	C, a/B = 0.4	C, a/B = 0.6	C, a/B = 0.8
0.2	0°	0.617	0.724	0.899	1.190
	45°	0.990	1.122	1.384	1.657
	90°	1.173	1.359	1.642	1.851
0.4	0°	0.767	0.896	1.080	1.318
	45°	0.998	1.075	1.247	1.374
	90°	1.138	1.225	1.370	1.447
0.6	0°	0.916	1.015	1.172	1.353
	45°	1.024	1.062	1.182	1.243
	90°	1.110	1.145	1.230	1.264
1.0	0°	1.174	1.229	1.355	1.464
	45°	1.067	1.104	1.181	1.193
	90°	1.049	1.062	1.107	1.112

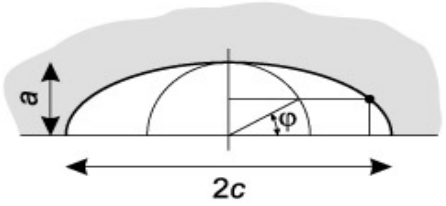

Raju I.S.,Newman J.C. Jr. Stress Intensity Factors for Two Symmetric Corner Cracks, Fracture Mechanics, ASTM STP 677, pp. 411-430 (1979).

SUPERPOSITION OF STRESS INTENSITY FACTORS

1) Crack under Internal Pressure:

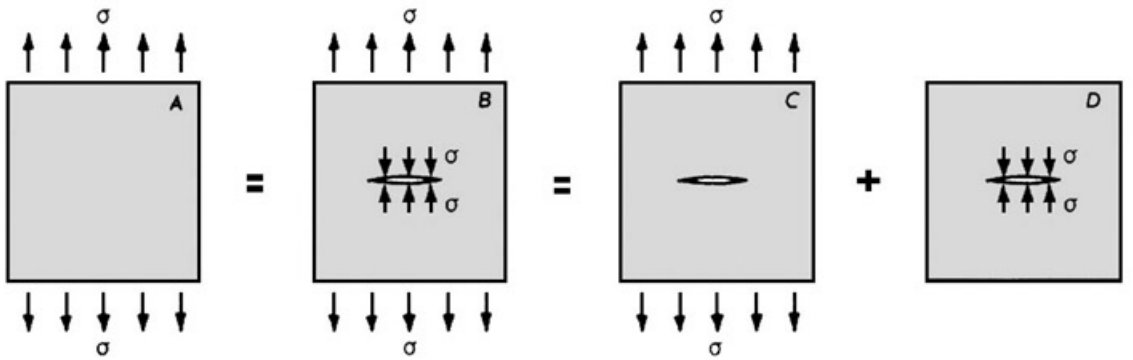

$$K_I^A = K_I^B = K_I^C + K_I^D = 0 \Longrightarrow K_I^D = -K_I^C = -\sigma\sqrt{\pi a} \qquad P = -\sigma \rightarrow \boxed{K_I^P = P\sqrt{\pi a}}$$

Semi-elliptical surface crack in a cylindrical pressure vessel:

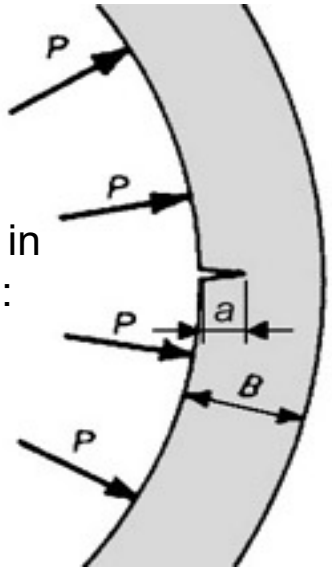

$$\sigma_H = P\frac{R}{B} \rightarrow K_I^{\sigma_H} = \frac{C\sigma_H\sqrt{\pi a}}{\Phi} = \frac{CPR\sqrt{\pi a}}{B\,\Phi}$$

$$K_I^P = \frac{CP\sqrt{\pi a}}{\Phi}$$

$$\boxed{K_I = K_I^{\sigma_H} + K_I^P = \frac{CP\left(1+\frac{R}{B}\right)\sqrt{\pi a}}{\Phi}}$$

CRACK TIP PLASTICITY

First approximation:

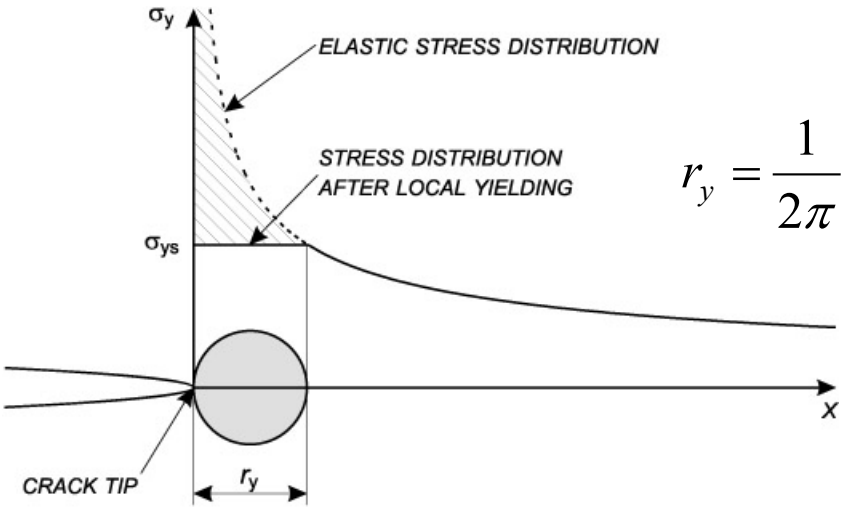

$$r_y = \frac{1}{2\pi}\left(\frac{K}{\sigma_{YS}}\right)^2$$

Better approaches

-selected shape: better size estimation

-Irwin

-Dudgale

-Better shape but first order approximation for the size

Irwin approach: - stress redistribution; elastic – plastic; plane stress

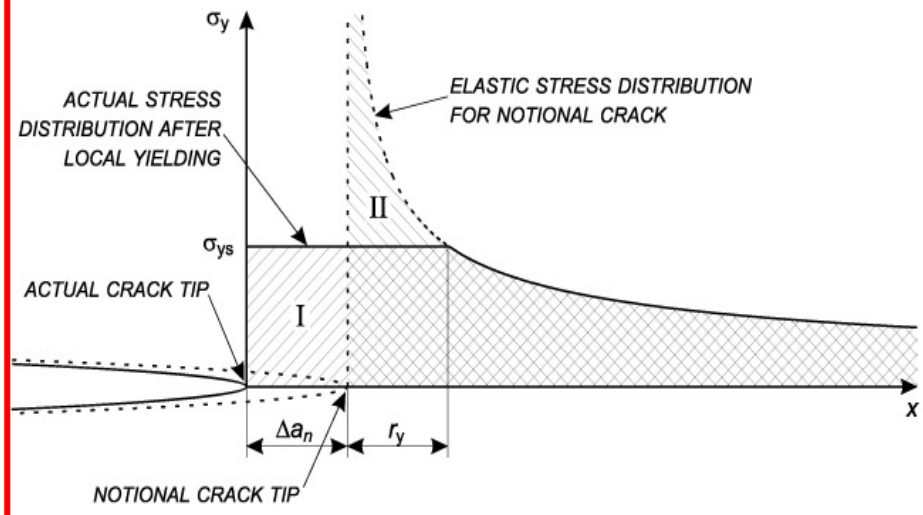

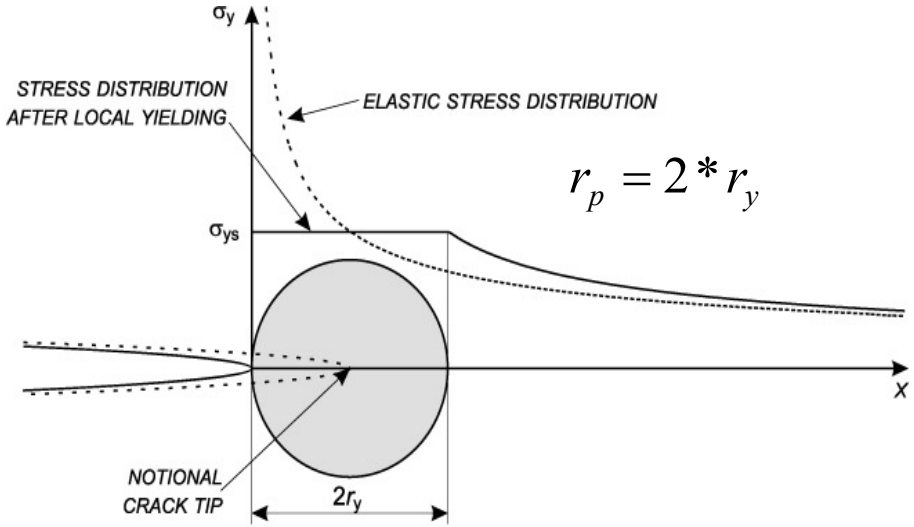

$$r_p = 2 * r_y$$

First Order Aproximations of **Plastic Zone Shapes**

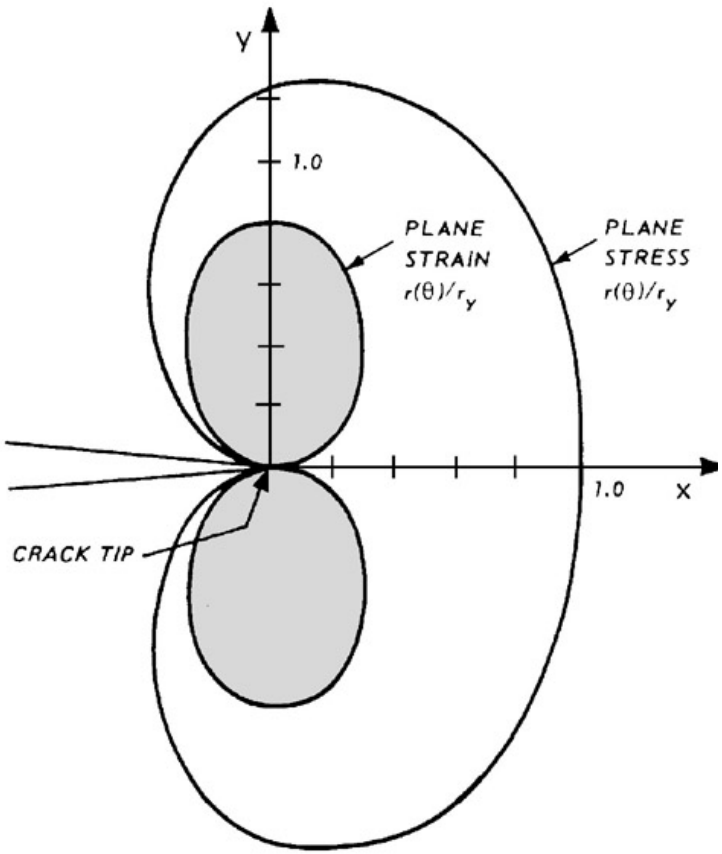

Plastic zone shape from Von Mises yield criterion

Through-thickness plastic zone in a plate of intermediate thickness

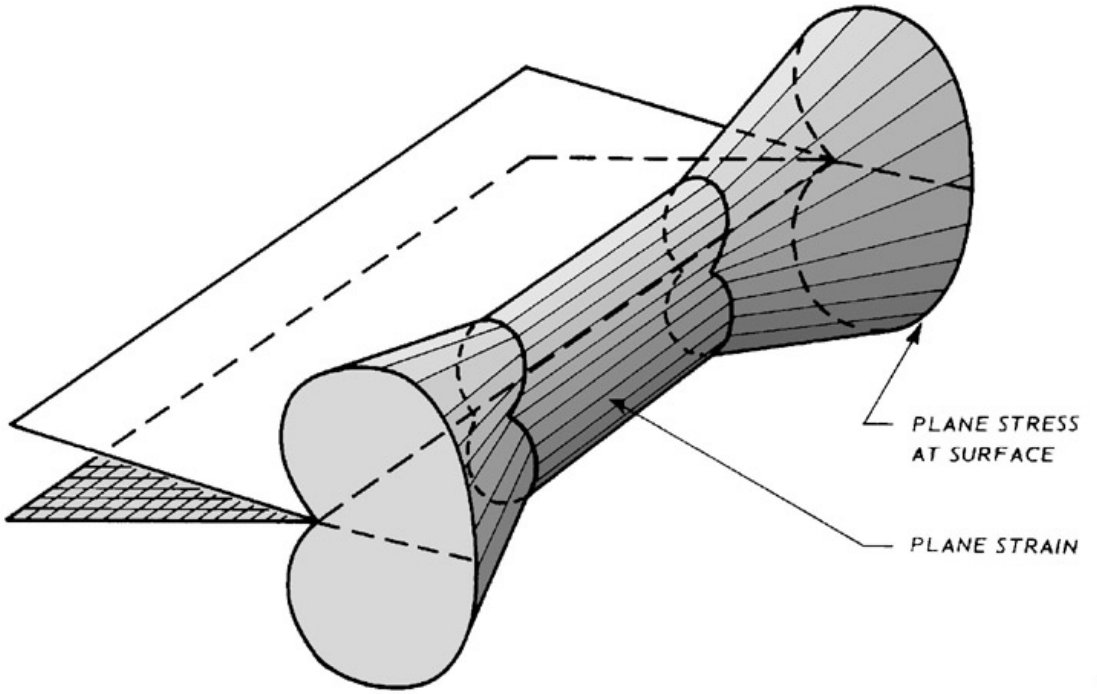

Empirical Rules to estimating Plane Stress vs. Plane Strain conditions:

-Plane Stress: $2r_y \approx B$

-Plane Strain: $2r_y < 1/10\ B$

FRACTURE TOUGHNESS

Is K a useful parameter to characterise fracture toughness?

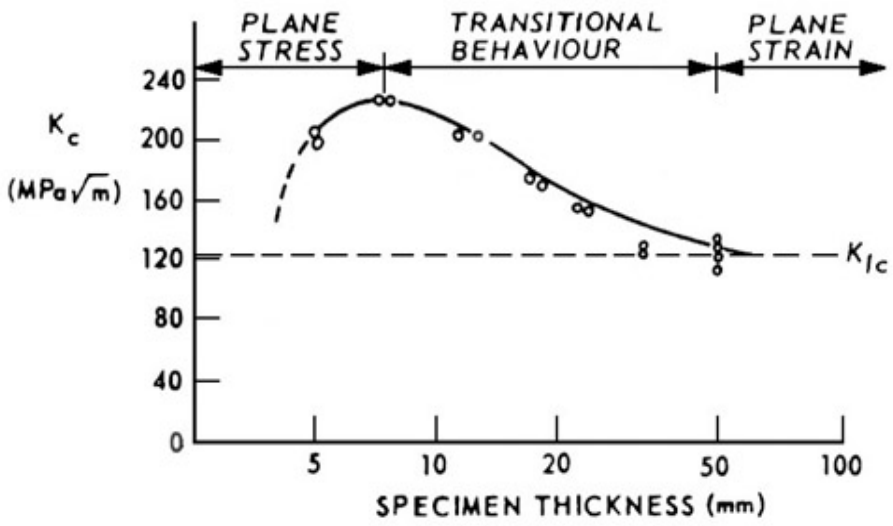

Variation in K_C with specimen thickness in a high strength maraging steel

Under conditions of:

- small scale plasticity
- plane strain

$Kc = K_{IC}$

K_{IC} is a material property: **fracture toughness of linear elastic materials**

Effect of Specimen Thickness on Mode I Fracture Toughness

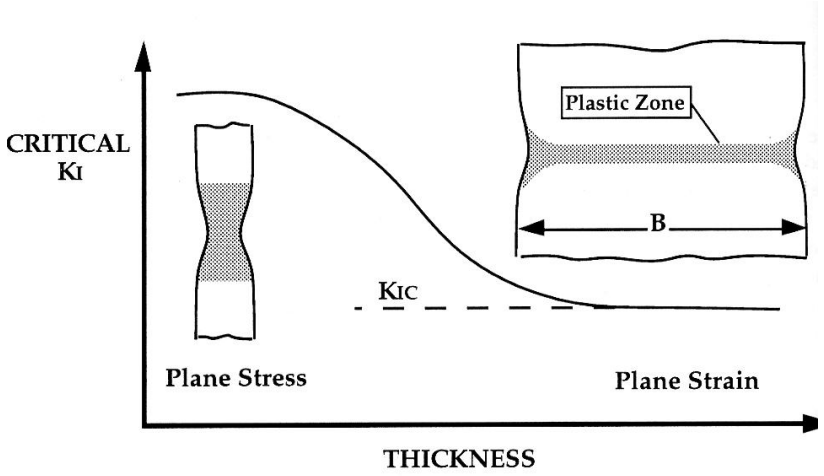

Limits to the Validity of LEFM:

After considerable experimental work the following minimum specimen size requirements were established to be in a condition of :

- plane strain
- small scale plasticity

$$a, \mathrm{B}, (\mathrm{W}-\mathrm{a}) \geq 2.5\left(\frac{K_{IC}}{\sigma_{YS}}\right)^2$$

$$a, \mathrm{B}, (\mathrm{W}-\mathrm{a}) \geq 2.5 * 2\pi * \frac{1}{2\pi}\left(\frac{K_{IC}}{\sigma_{YS}}\right)^2 = 2.5 * \pi * 2r_y \approx 8 * (2r_y)$$

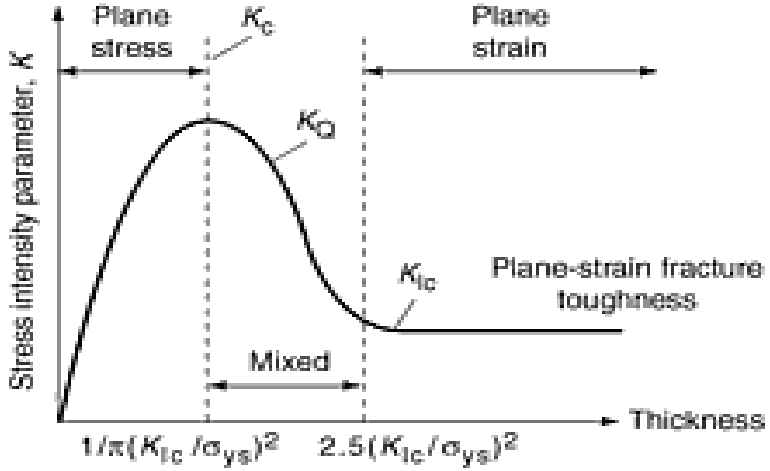

$$r_y = \frac{1}{2\pi}\left(\frac{K}{\sigma_{YS}}\right)^2$$

LEFM Testing: ASTM E-399, committee E8 Fatigue and Fracture

Fatigue pre-cracked specimens !

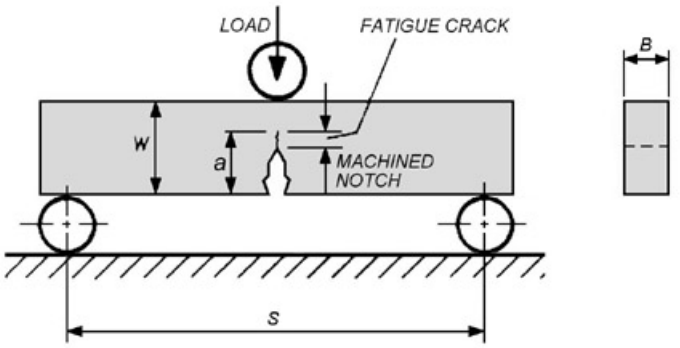

B = 0.5 W
S = 4 W
a = 0.45-0.55 W

$$K_I = \frac{LOAD * S}{B * W^{3/2}} * f\left(\frac{a}{W}\right)$$

where

$$f\left(\frac{a}{W}\right) = \frac{3\left(\frac{a}{W}\right)^{1/2}\left[1.99 - \frac{a}{W}\left(1-\frac{a}{W}\right)\left\{2.15 - 3.93\left(\frac{a}{W}\right) + 2.7\left(\frac{a}{W}\right)^2\right\}\right]}{2\left(1+2\frac{a}{W}\right)\left(1-\frac{a}{W}\right)^{3/2}}$$

ASTM Standard Single Edge notched Bend (**SENB**) Specimen

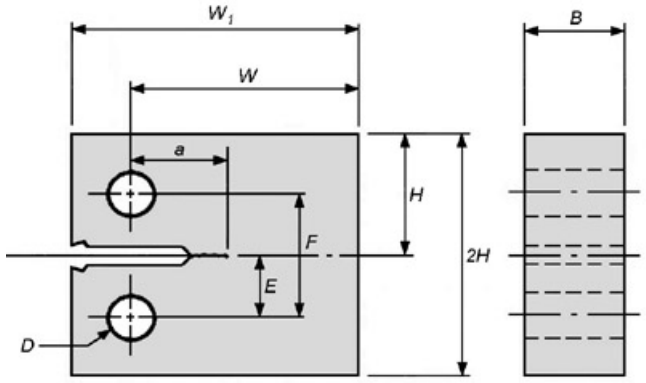

B = 0.5 W
H = 0.6 W
W1 = 1.25 W
F = 2E = 0.55 W
D = 0.25 W
a = 0.45-0.55 W

$$K_I = \frac{LOAD}{B * W^{1/2}} * f\left(\frac{a}{W}\right)$$

where

$$f\left(\frac{a}{W}\right) = \frac{\left(2+\frac{a}{W}\right)\left\{0.886 + 4.64\left(\frac{a}{W}\right) - 13.32\left(\frac{a}{W}\right)^2 + 14.72\left(\frac{a}{W}\right)^3 - 5.6\left(\frac{a}{W}\right)^4\right\}}{\left(1-\frac{a}{W}\right)^{3/2}}$$

ASTM Standard Compact Tension (**CT**) Specimen

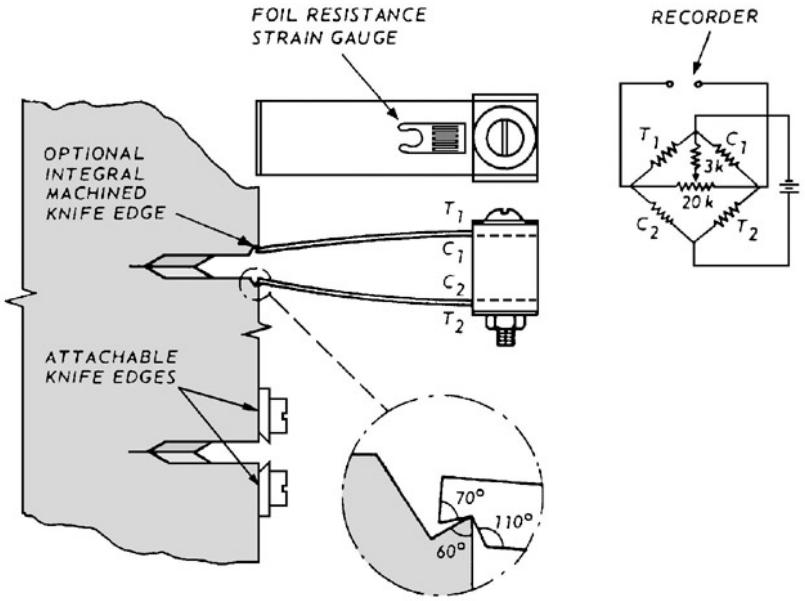

Clip gauge and ist attachment to the specimen

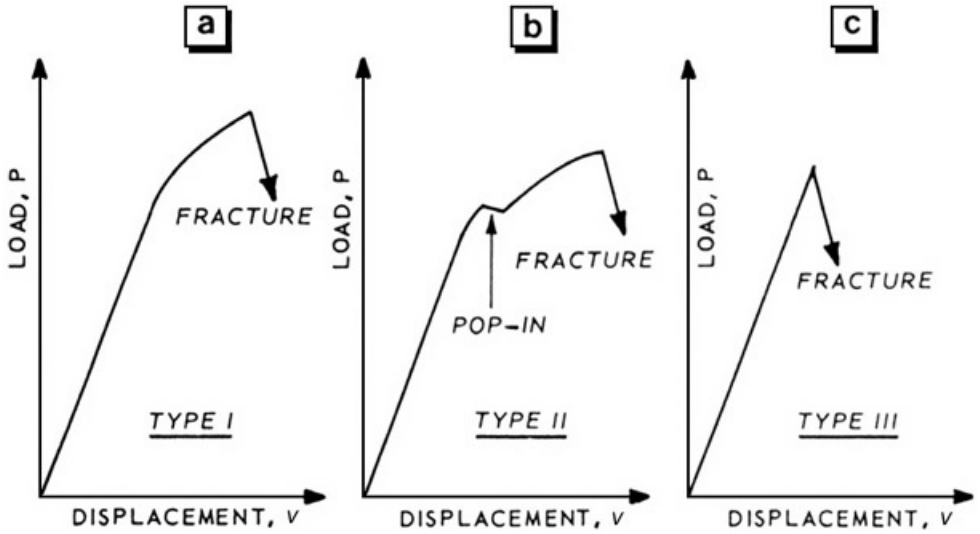

Principal types of load-displacement plots obtained during KIC testing

ANALYSIS

-Line at 5% offset (95 % of tg OA equivalent to 2 % crack extension

- Ps: intersection 5 % offset with P-v record
- if there is a P value > Ps before Ps, then $P_Q = P_s$
- check if $P_{max} / P_Q < 1.10$, then
- go to K(P_Q): calculate K_Q (conditional K_{IC})
- check if for K_Q the specimen size requirements are satisfied, then
- check if crack front is symmetric, then

$K_Q = K_{IC}$ (valid test)

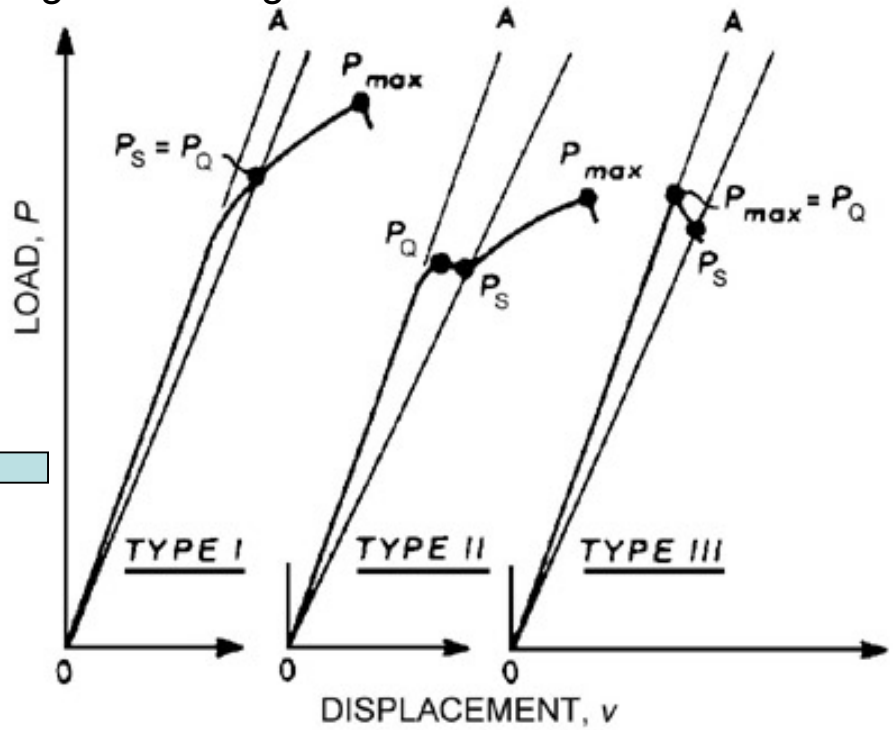

Material Toughness Anisotropy

To provide a common scheme for describing material anisotropy, ASTM standardized the following six orientations:

L-S, L-T, S-L, S-T, T-L, and T-S.

The first letter denotes the direction of the applied load; the second letter denotes the direction of crack growth. In designing for fracture toughness, consideration of anisotropy is very important, as different orientations can result in widely differing fracture-toughness values.

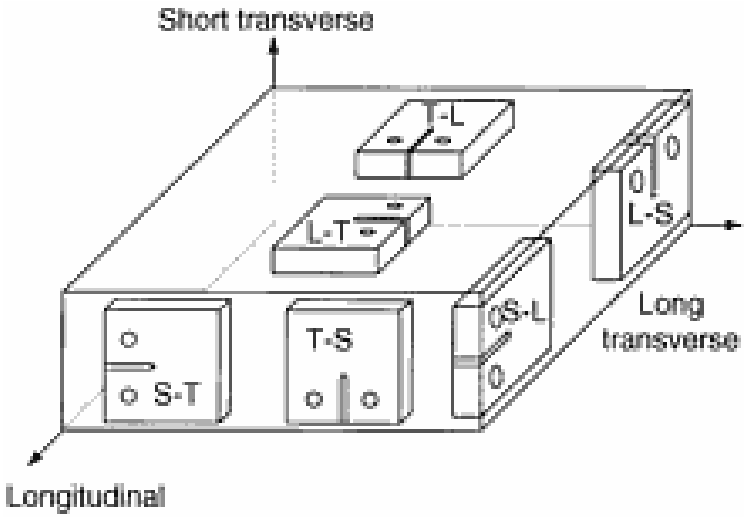

Alloy	σY [MPa]	Orient.	T [°C]	KIC [Mpa $m^{1/2}$]
2042-T351	385	L-T	29	31
2024-T351	292	S-L	32	21
7075-T651	530	L-T	28	32
7075-T651	446	S-L	29	21
4140	1379	L-T	24	65
4140	1586	L-T	24	55
4340	1455	L-T	21	83
Ti-6Al-4V	889	L-T	24	64
Ti-6Al-4V	910	T-L	24	68
Ti-6Al-4V	883	S-L	24	75

When the crack plane is parallel to the rolling direction, segregated impurities and intermetallics that lie in these planes represent easy fracture paths, and the toughness is low. When the crack plane is perpendicular to these weak planes, decohesion and crack tip blunting or stress reduction occur, effectively toughening the material. On the other hand, when the crack plane is parallel to the plane of these defects, toughness is reduced because the crack can propagate very easily.

Introduction to Structural Integrity

- Practical application of fracture mechanics is based on twofold interpretation of its parameters: on one hand, they represent loading and structural geometry, and on the other they represent material properties and its resistance to crack growth.
- In that way the triangle of fracture mechanics has been established, Fig. 1, enabling fracture mechanics to become one of the foundations of a new discipline – structural integrity. Thus, instead of only handling fracture analysis, fracture mechanics has become an important tool in the hands of engineers whose job is to prevent fracture.

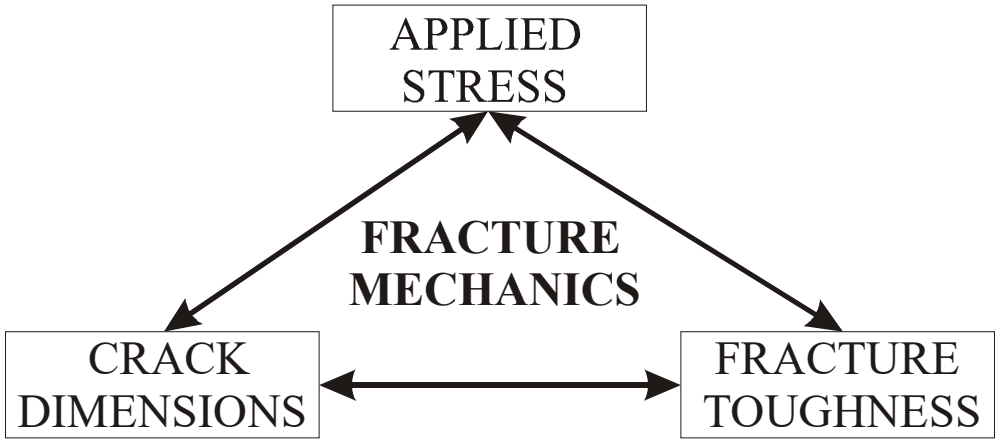

Figure 1. Fracture mechanics triangle

Introduction –Alaska pipeline case

- Fracture mechanics has brought significant changes in engineering practice. As an example to illustrate this statement, the problem with the Alaska pipeline and application of the fracture-safe principle in design may be mentioned. In case of the pipeline from Alaska to the rest of the USA, the fracture mechanics criteria were adopted instead of traditional standards on acceptable defects in a welded joint.
- Namely, when non-destructive testing revealed a large number of defects in round welded joints which, according to the then effective standards, should have been repaired, the question of economic justification, i.e. necessity of repair, arose.
- Therefore, the institution in charge, following the requirement of the company that installed the pipeline, addressed to the National Institute of Standards and Technology (then the National Bureau of Standards – NBS) for help.
- Detailed analysis of fracture mechanics parameters, based on the concept of crack tip opening displacement, covered assessment of the crack growth driving force on one hand, and resistance of the material (weld metal) to crack growth on the other hand. The results of that research were officially accepted, so that the scope of repair was dramatically reduced, due to which unnecessary costs were avoided as well as risks of occurrence of new defects caused by repair welding.

Introduction

- Thanks to that research it was concluded that the analysis of fracture mechanics is an acceptable base for admissible exception from the existing standards under certain circumstances, if such analysis provides convincing and conservative (safe) assessment of structural integrity. It should also be emphasized that this level of application of fracture mechanics was reached not only through this detailed investigation, but also through preceding intensive development as a scientific discipline.
- It is thus obvious that the fundamental change that fracture mechanics has brought into engineering practice is the recognition of the fact that existence of cracks and similar defects cannot be avoided, and that their effects on structural integrity should be analysed.
- In practice, it also frequently happens that methods of non-destructive tests (NDT) reveal a crack or a similar defect in a structure, for which critical stress is then defined, based on known fracture toughness of the material, or either the minimal fracture toughness of the material is subsequently defined based on the stress state of a structure. This concept can be applied already in the phase of structural design, if one assumes existence of cracks, dimensions of which correspond to the sensitivity of the NDT equipment.

Application of linear elastic fracture mechanics

The application of LEFM is based on the stress intensity factor, K_I, which on one hand represents loading and structural geometry, including crack dimensions, and on the other, its critical value, K_{Ic}, represents the material property. Based on this interpretation of LEFM parameters and Griffith's energy criterion, one can establish simple dependencies for the assessment of structural integrity.

$K_I \leq K_{Ic}$ structural integrity is not threatening,

$K_I > K_{Ic}$ structural integrity is jeopardized due to eventual brittle fracture.

Application of elastic plastic fracture mechanics

There are few ways to take into account material plasticity in assessment of structural integrity, all of which are based on application of crack tip opening displacement or J integral, as appropriate parameters of elastic-plastic fracture mechanics.

Crack tip opening displacement (CTOD), although without clear theoretical base, has a wide practical application, mainly due to the simplicity of determination. On the other hand, the J integral requires a more complex procedure for determination, but as an energy parameter based on fundamental laws of continuum mechanics has equally important practical application.

Failure analysis diagram

Structures made of ductile materials are less susceptible to brittle fracture, and therefore may fracture by plastic collapse. The mechanism of plastic collapse is not covered by designed CTOD curve, so its analysis requires a more general, two-parameter approach, realized through the Failure Analysis Diagram (FAD). This diagram represents the limit curve, constructed according to the modified model of a yielding strip for a passing-through crack on an infinite plate:

$$\frac{K_{eff}}{K_{\mathrm{I}}} = \frac{\sigma_c}{\sigma}\left[\frac{8}{\pi^2}\ln\sec\frac{\pi}{2}\frac{\sigma}{\sigma_c}\right]^{1/2}$$

where $K_{\mathrm{I}} = \sigma\sqrt{\pi a}$, K_{eff} was introduced instead of δ ($K_{eff}^2 = \delta\sigma_Y E$), and yield stress σ_Y was replaced by plastic collapse stress σ_c as a more convenient yield criterion for actual structures. As a final step, non-dimensional variables $S_r = \sigma/\sigma_c$ and $K_r = K_{\mathrm{I}}/K_{\mathrm{I}c}$ are defined, where it is supposed that K_{eff} equals to the fracture toughness of the material:

$$K_r = S_r\left[\frac{8}{\pi^2}\ln\sec\left(\frac{\pi}{2}S_r\right)\right]^{-1/2}$$

Failure analysis diagram

If the material is completely ductile, the structure fails due to plastic collapse at $S_r = 1$, while for fracture of a completely brittle material $K_r = 1$. In all other cases there is an interaction between plastic collapse and brittle fracture, so that K_r and S_r are less than 1, and pairs of corresponding values make a boundary curve.

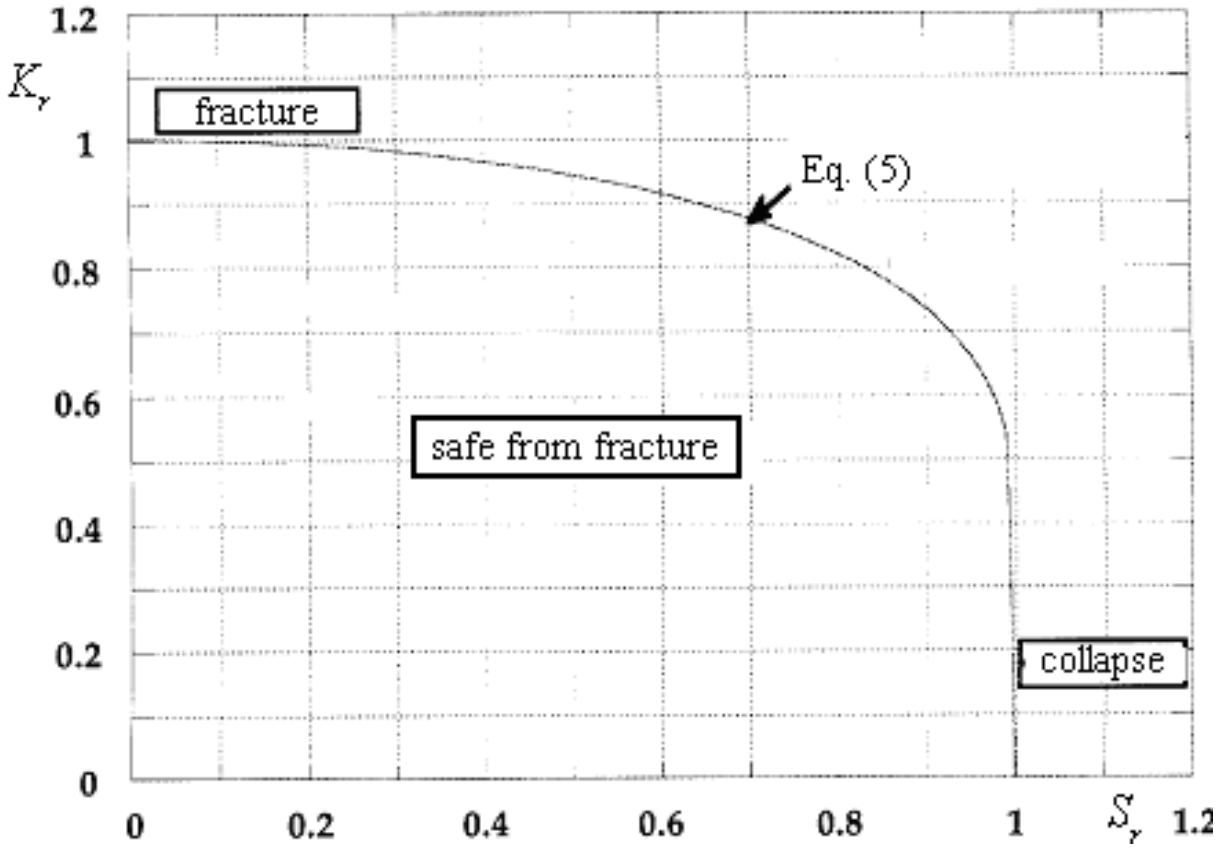

Pressure vessels at hydroelectric power plant “Bajina Bašta”

- This example is a typical problem when regular control of NDT reveals ‘unacceptable’ defects according to standard ISO 5817, as was the case with welded joints of vessels for compressed air in hydroelectric power plant ‘Bajina Bašta’.

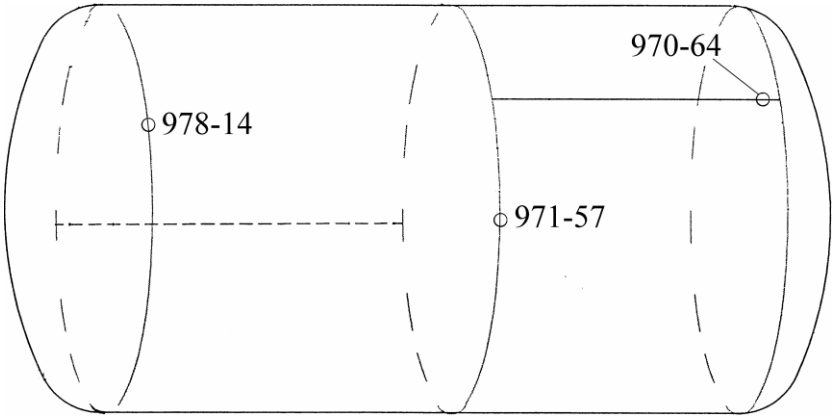

- The vessel No. 970 had two defects marked as ‘unacceptable,’ one of which from the photo 970-64, was again ultrasonically examined, which was definitely confirmed as incomplete penetration 60 mm long and 2 mm wide. By defect length, in this case, is to be understood the dimension in the direction of longitudinal welded joint, near the upper circular seam, while the width of the defect is its size in the direction of weld thickness. This defect was chosen as one of three ‘critical,’ both because of dimensions and location, the other two being 971-57 and 978-14.

Pressure vessels at hydroelectric power plant “Bajina Bašta”

- As far as dimensions are concerned, defect 970-14 was the largest one, and potentially the most dangerous, because of its location, as it spread near the change from cylindrical shell to torus–spherical dish cover, where local bending may exists.
- Vessel No. 971 had 11 defects marked unacceptable, according to Report No. 2/98 of Goša Institute, among which defect from Photo No. 971-57 was chosen as critical, the lack of side wall fusion 10 mm long, located in central circular welded joint. Detailed ultrasonic inspection did not reveal this defect, but it was still taken into account.
- Vessel No. 978 had 5 defects marked as unacceptable, out of which the incomplete penetration, 25 mm long, from Photo No. 978-14 was chosen as the critical one, although additional ultrasonic inspection failed to register it. The width of this defect, the value of 2 mm was adopted that, according to the documentation of vessel No. 978, corresponded to the predicted size of the weld metal root, and at the same time was the upper sensitivity limit for ultrasonic examination.

The analysis of critical defects using methods of fracture mechanics

- The defects marked as ‘critical’ were analyzed using methods of fracture mechanics, by applying conservative approach. Therefore, all three were considered as cracks: defects No. 970-64 and 978-14 as surface cracks (partially passing through the thickness, while defect No. 971-57 was considered a line crack (passing through the entire thickness). In this way an extremely conservative assessment was adopted for defect 971-57, in order to check the behaviour of the vessel, even in such a case.
- In order to determine stress intensity factors, one should know the external loading and geometry. Fracture toughness in this case could not have been determined and conservative assessment of its value was used instead. Care was also taken for the possibility of corrosion and fatigue, as well as of effects of residual stresses and the vicinity of dish cover, or openings. The analysis of ‘critical’ defects is given herein.

The analysis of critical defects using methods of fracture mechanics

- The data, essential for the analysis of defect No.970-64 are as follows:
  - vessel geometry (thickness t = 50 mm, mean diameter D = 2150 mm);
  - material of vessel cylindrical shell: NIOVAL 50 (low-alloyed steel of increased strength)
  - crack geometry (60 mm long, 2 mm wide, direction–along the weld, location–root of longitudinal weld metal, adjacent to the circular weld–dish cover connection, far away from the openings);
  - loading (internal pressure) p = 81 bar, residual stress σ_R = 200 MPa–the highest value – transversal to weld, based on experience with similar material and vessel;
  - weld metal fracture toughness is 1580 MPa$\sqrt{}$mm, as minimum value.

The analysis of critical defects using methods of fracture mechanics

- Having in mind the conservative approach in the analysis of critical defects, it has been assumed that defect No. 970-64 spreads over the entire length of the cylindrical part of vessel.
- In that case, problem is observed in the section transversal to longitudinal direction of vessel, where the influence of the curve is negligible (justifiable for 50 mm thickness and diameter of 2150 mm). The crack dimension, defined as 60 mm length exists no more in the analysis and the dimension so far defined as width becomes the length (2 mm).

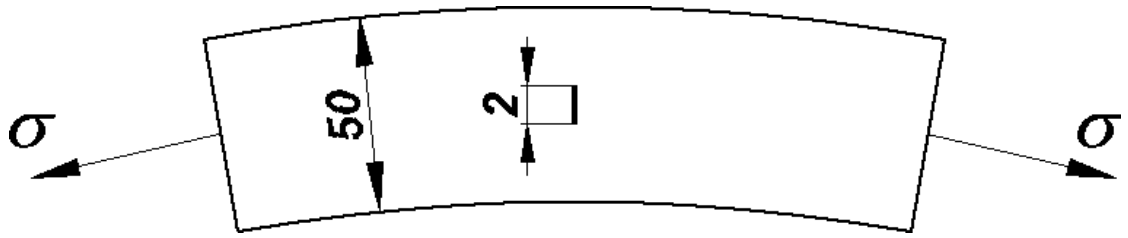

The analysis of critical defects using methods of fracture mechanics

- If we assume that the remote stress is a sum of circumferential stress induced by internal pressure ('boiler formula') and cross-sectional residual stress in the middle of a weld, the following is obtained for the stress intensity factor:

$$K_{\mathrm{I}} = \left(\frac{pR}{t} + \sigma_R \right) \sqrt{\pi a} = \left(\frac{8.1 \cdot 1075}{50} + 200 \right) \sqrt{\pi} = 663 \ \mathrm{MPa}\sqrt{\mathrm{mm}}$$

- Having in mind that the obtained value of K_{I} is only 42% of a minimal value of $K_{\mathrm{I}c}$ (1580 MPa√mm), it may be concluded that there is no risk of brittle fracture. This conclusion is also valid even if one assumes the crack length to be twice of the measured (thus taking into account measuring inaccuracy), since in that case K_{I} = 937 MPa√mm, which is 59% of the minimal value of $K_{\mathrm{I}c}$, still providing sufficient safety against brittle fracture.

The analysis of critical defects using methods of fracture mechanics

- Defect No. 978-14 (incomplete penetration, 25 mm long and 2 mm wide, in a circular weld connecting the lower dished cover) is presented as a surface crack, but it is assumed for this crack too, that it spreads over the entire circumference of the vessel. The data essential for analysis (with the same material as in previous analysis) are:
  - vessel geometry (thickness t = 42 mm, mean diameter D = 1958 mm);
  - crack geometry: 25 mm long, 2 mm wide, direction–along the weld, location: root of circular weld metal connecting the dish cover, far from the openings;
  - loads (internal pressure p = 78 bar, residual stress σ_R = 200 MPa, the same as with defect No. 970-64).

The analysis of critical defects using methods of fracture mechanics

- In this case the problem is observed in the section transversal to circumferential direction of the vessel. The section is presented simplified, since even the part belonging to the cover is shown as a plane, justly disregarding curve effects.
- Moreover, it is ignored that the stress in the torus part of the cover differs from the stress in a cylindrical part of the vessel, since in the torus area adjacent to the cylindrical part the stress is pressure, and not dangerous for crack growth. Thus, non-symmetry in the problem, caused by the location of crack is ignored, and same as in the previous case.

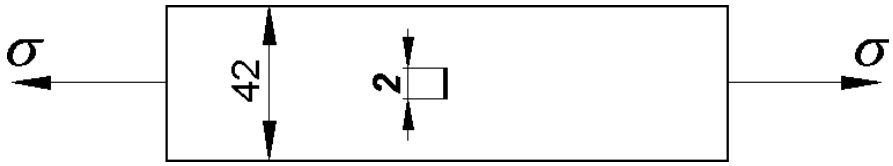

The analysis of critical defects using methods of fracture mechanics

If the sum of longitudinal stress, caused by internal pressure ('boiler formula'), and transversal residual stress in the centre of the seam is assumed to be the remote stress, than the following is obtained for stress intensity factor:

$$K_{\mathrm{I}} = \left(\frac{pR}{2t} + \sigma_R \right) \sqrt{\pi a} = \left(\frac{7.8 \cdot 979}{84} + 200 \right) \sqrt{\pi} = 515 \ \mathrm{MPa}\sqrt{\mathrm{mm}}$$

which is 32% of the critical value ($K_{\mathrm{I}c}$ = 1580 MPa$\sqrt{\mathrm{mm}}$), and does not threat the vessel. For twice this crack length,
K_{I} = 728 MPa$\sqrt{\mathrm{mm}}$ = 45%$K_{\mathrm{I}c}$ is obtained.

The analysis of critical defects using methods of fracture mechanics

- Defect No.971-57 (lack of penetration, 10 mm long, in a circular weld at the middle of the vessel) has from the very beginning been presented as a passing-through crack, as the other dimension remains unknown. The data important for the analysis are as follows:
  - pressure geometry (thickness t = 50 mm, mean diameter D = 2075 mm);
  - crack geometry (10 mm long, direction–along seam, location–circular weld metal in the middle of the vessel, far from the openings;
  - loads–internal pressure p = 81 bar, residual stress σ_R = 175 MPa – transversal to weld, away from weld centre, based on experience with similar material.

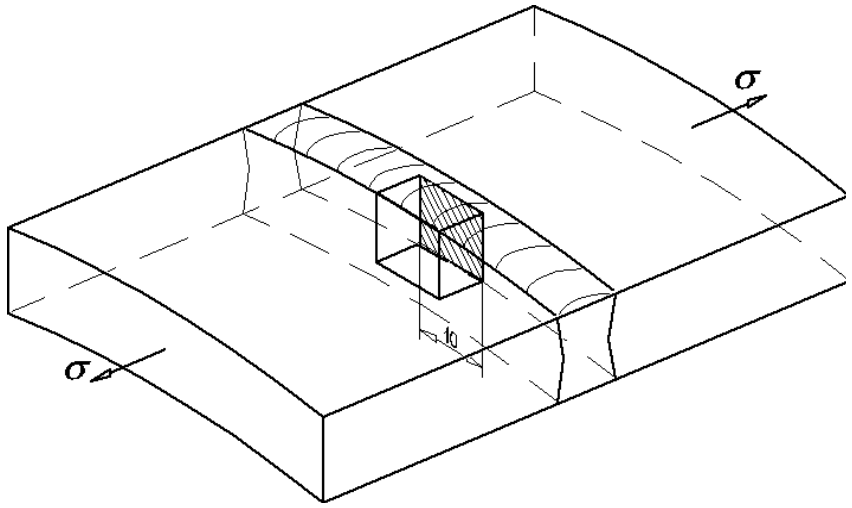

The analysis of critical defects using methods of fracture mechanics

As in the previous case, the problem is presented by a plate under tension, not in the cross section, but as a "separate" part of the cylinder. If the remote stress is assumed as a sum of the longitudinal, pressure induced stress ("boiler formula"), and the transversal residual stress, away from the weld centre, the stress intensity factor is:

$$K_{\mathrm{I}} = \left(\frac{pR}{2t} + \sigma_R \right) \sqrt{\pi a} = \left(\frac{8.1 \cdot 1075}{100} + 175 \right) \sqrt{5\pi} = 1039 \ \mathrm{MPa}\sqrt{\mathrm{mm}}$$

which is 66% of critical value ($K_{\mathrm{I}c}$ = 1580 MPa√mm). Even if one assumes twice the crack length, the stress intensity factor (K_{I} = 1465 MPa√mm for $2a$ = 20 mm) remains below critical value (92%).

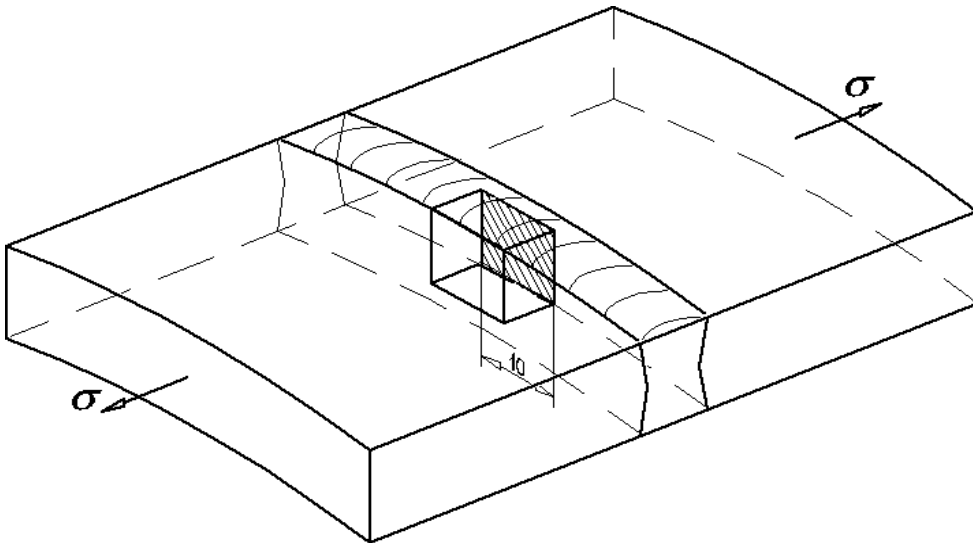

The analysis of critical defects using methods of fracture mechanics

Further analysis includes plastic material behaviour, i.e. the application of FAD. In that case the K_R parameter has already been defined: 0.59 for defect No.978-14 and 0.92 for defect No.971-57. For evaluation of the S_R parameter, one should define the stress in the net section from primary loading (internal pressure), while the secondary stress is not taken into account.

Net section stress for defect No. 970-64 is $\sigma_n = 1.08pR/t$, where the 1.08 factor takes into account the weakening of the 50 mm section thickness due to 4 mm long crack, so that the following is obtained:

$$S_R = \frac{\sigma_n}{\sigma_F} = 2\left(\frac{1.08\,pR}{t}\right)\Big/\left(R_{eH} + R_M\right) = 2\left(\frac{1.08 \cdot 8.1 \cdot 1075}{50}\right)\Big/\left(500 + 650\right) = 0.33$$

The stress in net section of defect No. 978-14 is $\sigma_n = 1.05pR/2t = 95$ MPa, with the section weakening coefficient of 1.05 (the 2 mm long crack for thickness of 42 mm), so that the following is obtained: $S_R = \frac{\sigma_n}{\sigma_F} = \frac{95}{575} = 0.17$

The analysis of critical defects using methods of fracture mechanics

- The influence of the vicinity of the dish cover is again taken to be negligible.
- The net section stress for defect No.971-57 is $\sigma_n = 1.05pR/2t = 87$ MPa, where section weakening coefficient is not taken into account as its influence is negligible, so that the following is obtained:

$$S_R = \frac{\sigma_n}{\sigma_F} = \frac{87}{575} = 0.15$$

- Based on values obtained for K_I/K_{Ic} and σ_n/σ_F, the points (0.33; 0.59), (0.17; 0.45), and (0.15; 0.92) are plotted in the failure analysis diagram (FAD), all located in the safe part of the diagram, Fig. 2.

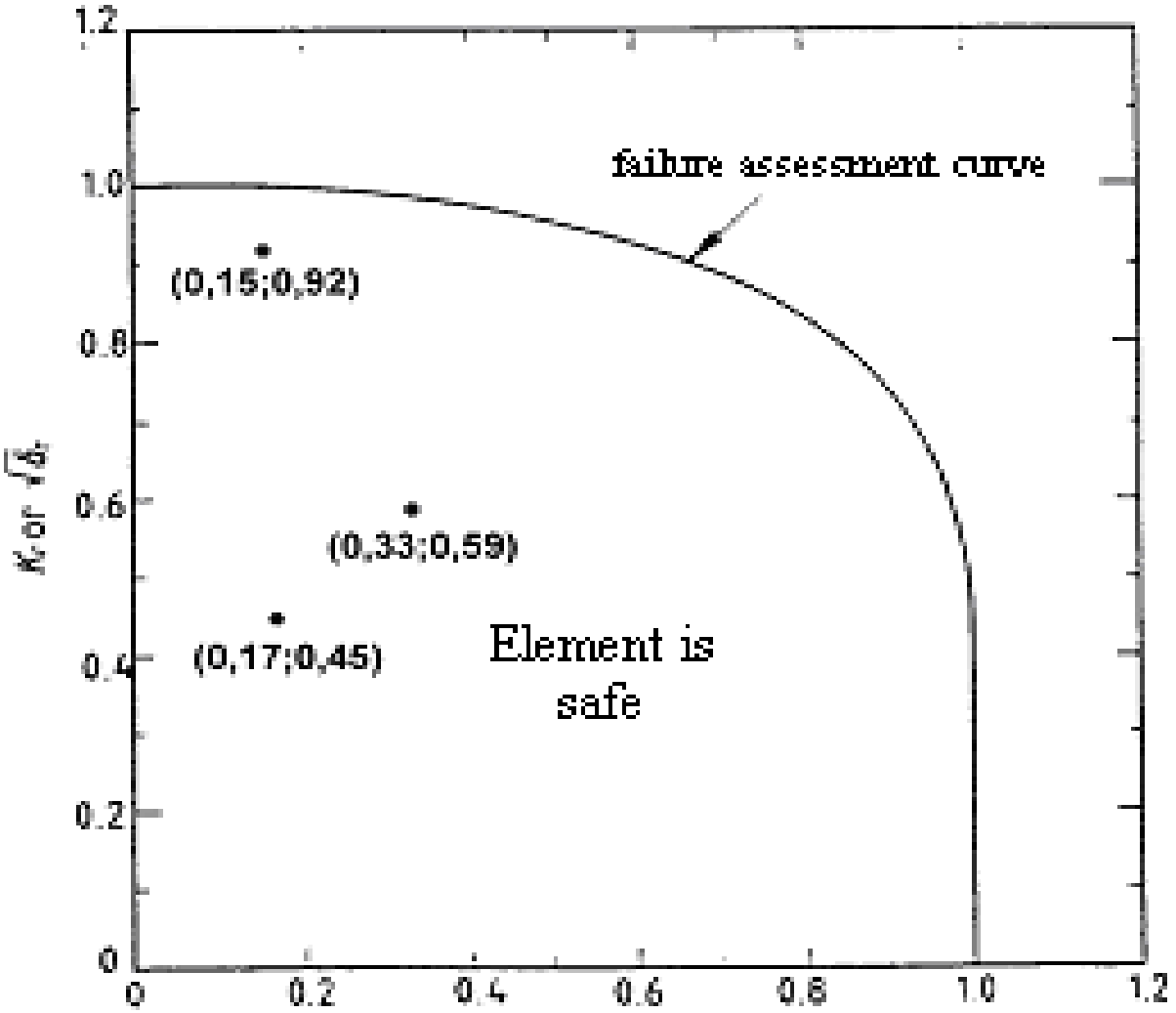

Figure 2. Failure assessment diagram for damaged vessels

Fracture Mechanics testing of PLA(X) material – Kic

Universal testing machine Shimadzu AGS-X 100kN

Tensile testing equipment

Pressure testing equipment

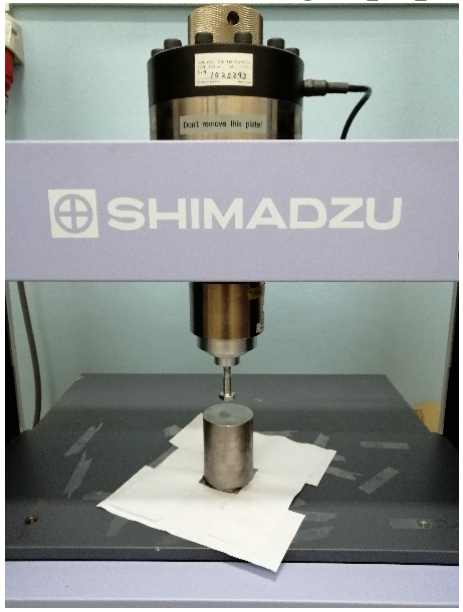

FDM printer / German RepRap X400 dual extruder

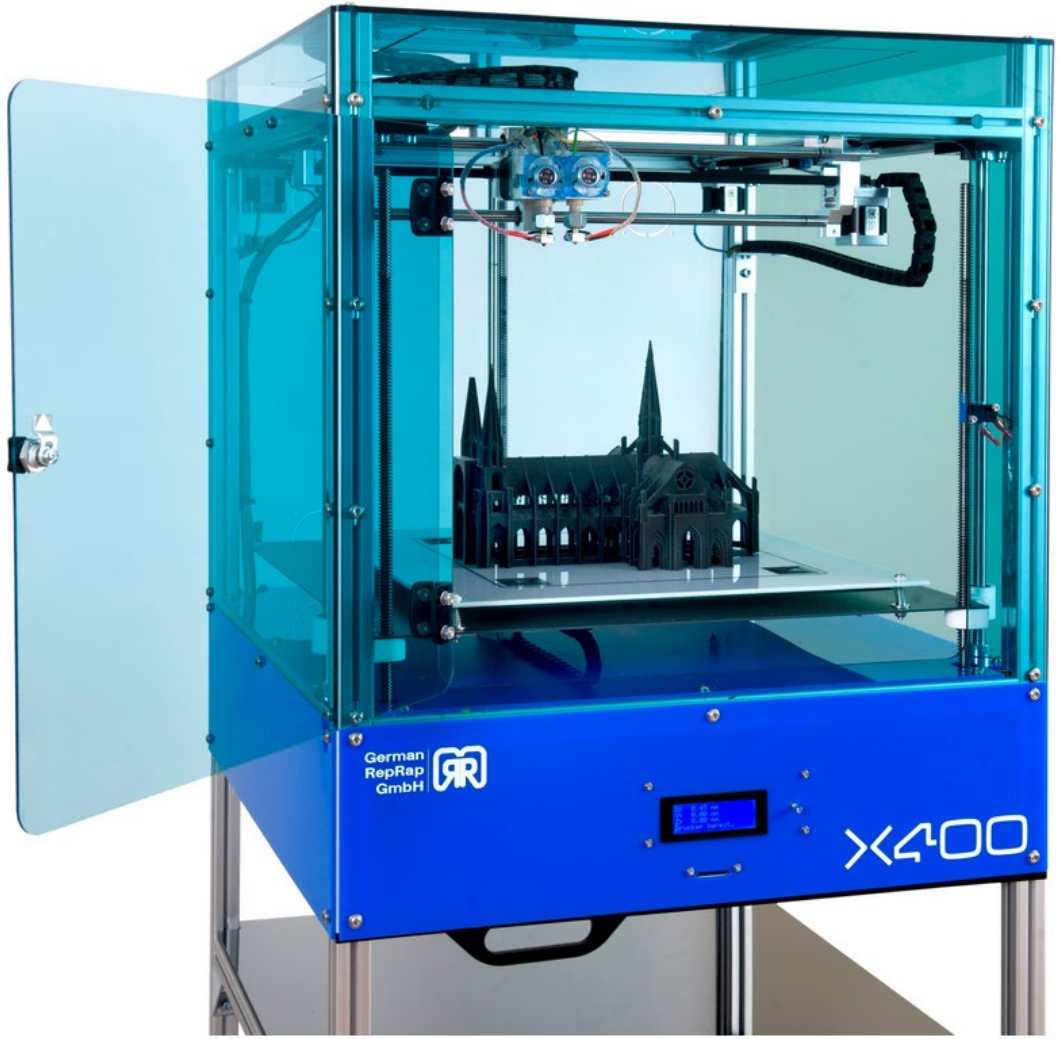

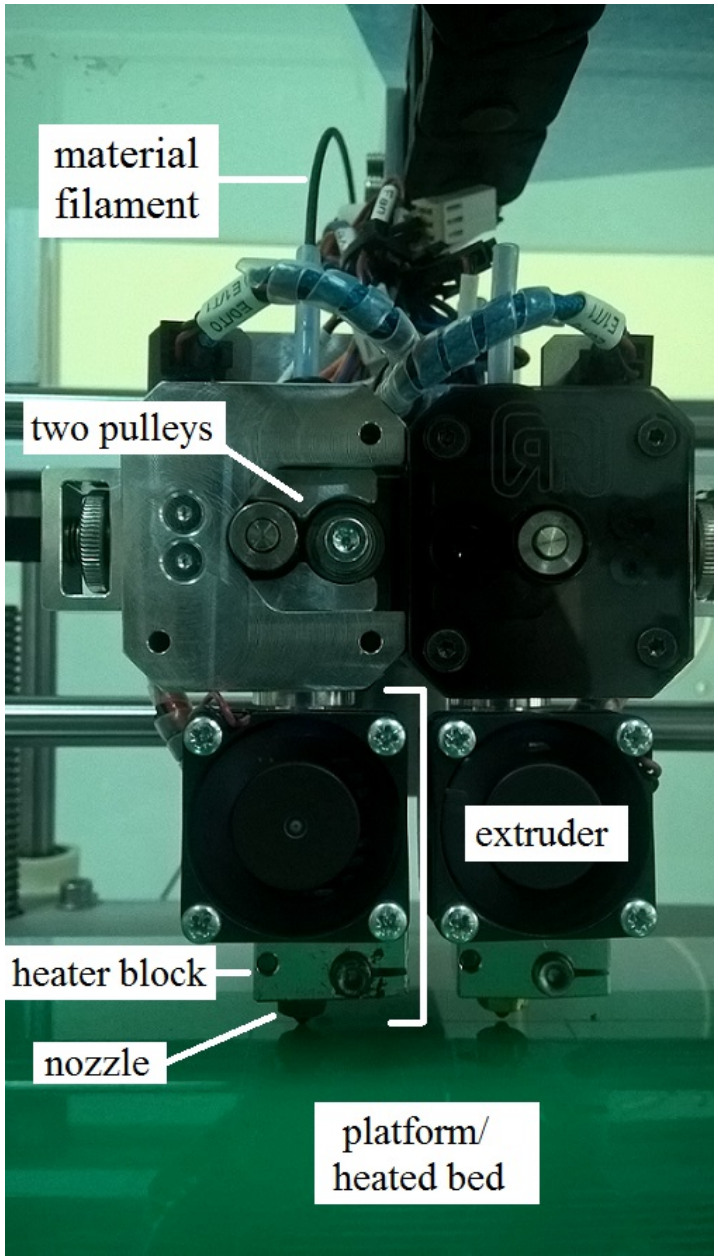

SLA printer FormLabs Form 2

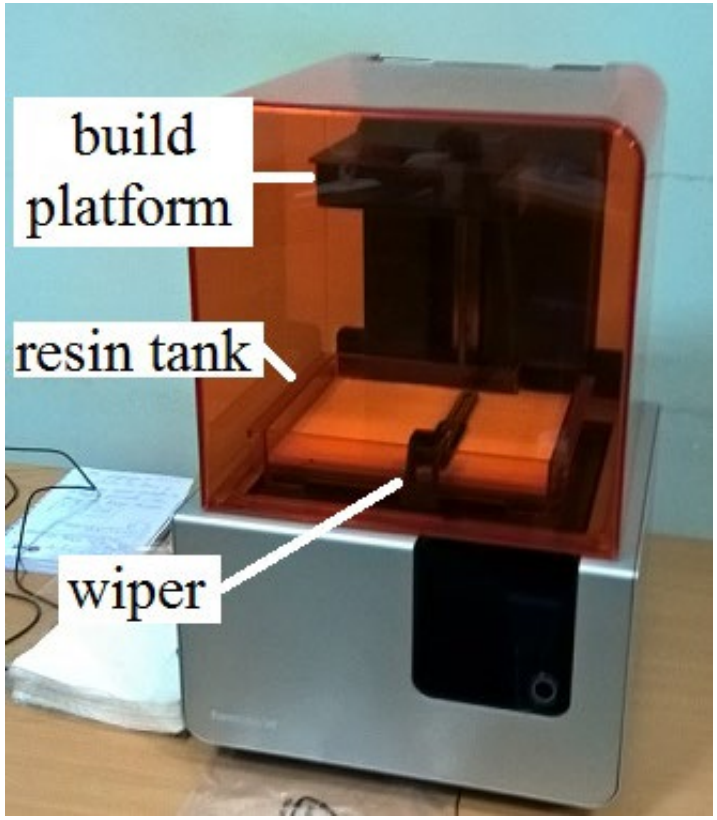

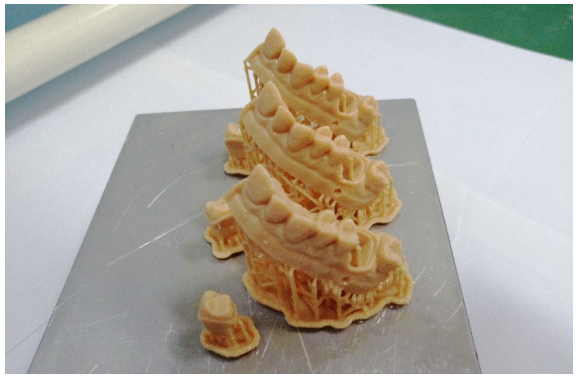

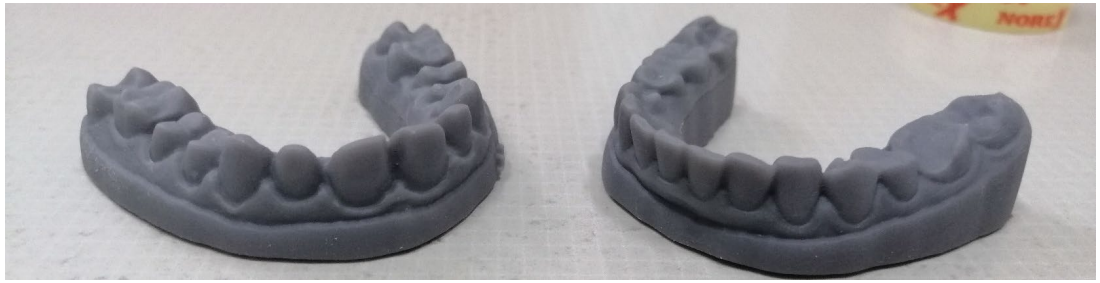

3D scanner Geomagic Capture

3D scanning work environment

Scanning head with rotating platform

Testing of PLA and PLAX - K_{Ic}

Diagramme F-delta for PLA tested in 3 Point Bend loading

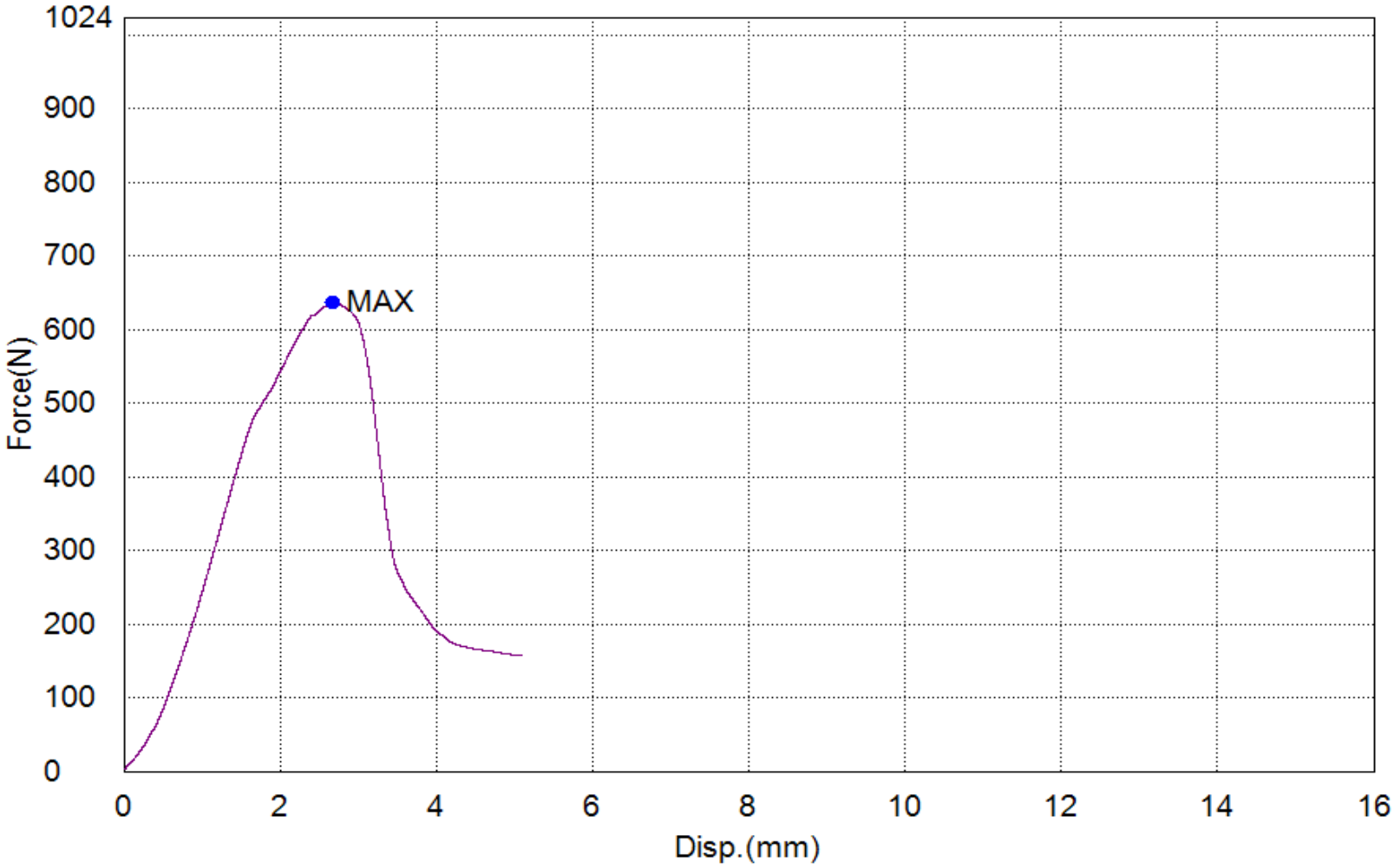

“Hand” calculation to get the first result! NOT VALID

D 5045 - 14 standard

SELB specimen

$B = 1\,cm$

$W = 2\,cm$

$a = 1\,cm$

$x = \frac{a}{W} = 0.5$

$f(x) = 10.65$

$$K_Q = \left(\frac{P_Q}{B W^{1/2}}\right) f(x)$$

4 specimens

$P_{Q_1} = 0.586\ kN$

$P_{Q_2} = 0.598\ kN$

$P_{Q_3} = 0.637\ kN$

$P_{Q_4} = 0.559\ kN$

$$K_{Q_1} = \left(\frac{0.586}{1 \cdot 1.41}\right) \cdot 10.65 = 4.42\ MPa\sqrt{m}$$

$K_{Q_2} = 4,51\ MPa\sqrt{m}$

$K_{Q_3} = 4,81\ MPa\sqrt{m}$

$K_{Q_4} = 4,22\ MPa\sqrt{m}$

$K_Q = K_{IC}$

$$B, a, (W-a) > 2.5\left(\frac{K_Q}{\sigma_Y}\right)^2 = 2.5\left(\frac{4.81}{55}\right)^2$$

$B, a, (W-a) > 0,0189\ m$

$> 18,9\ mm$

New set of specimens - redesigned

Details for one specimen

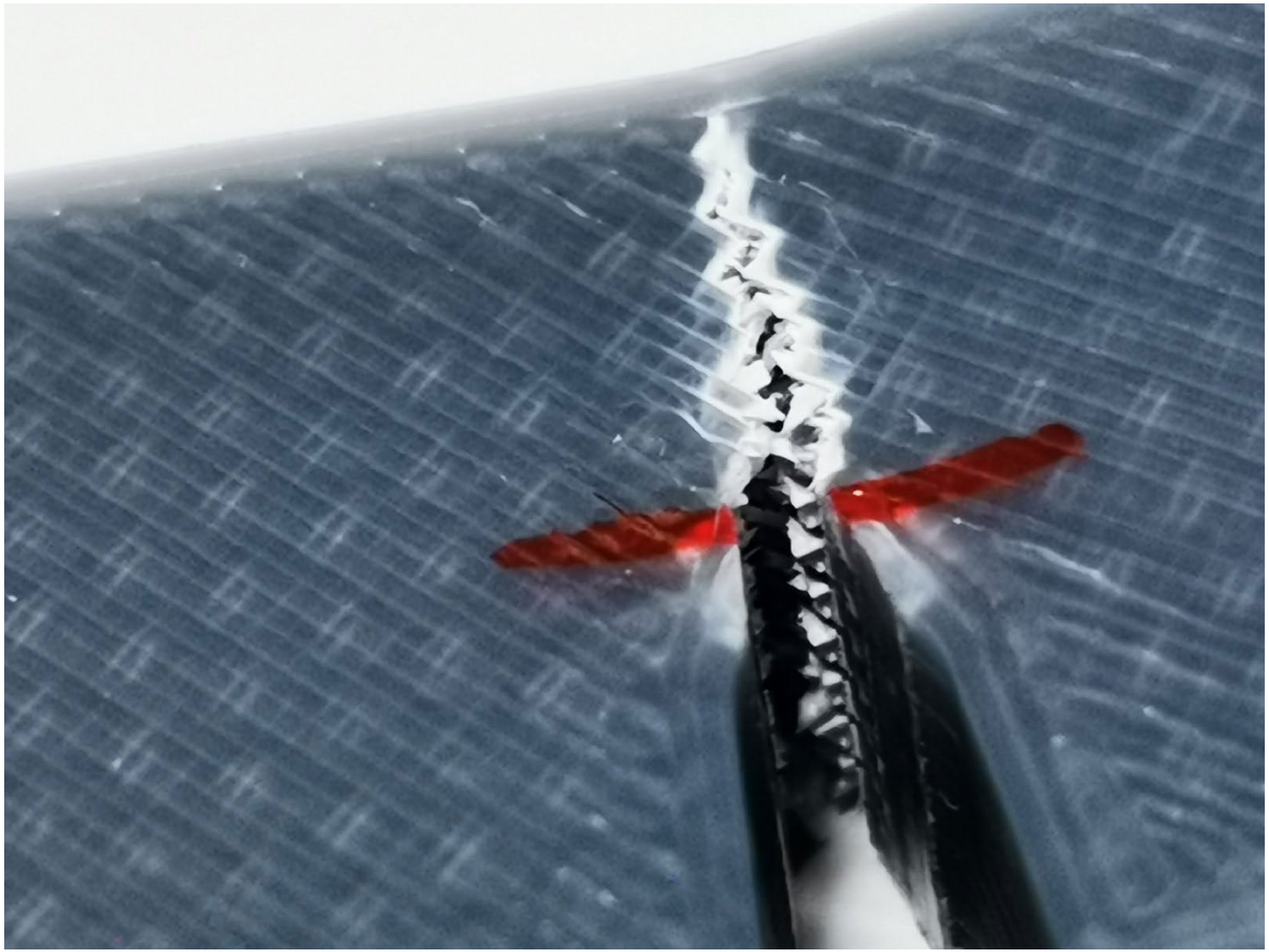

Valid results for KIc, between 2 and 2.5 MPa√m

Fatigue Crack Growth

Applications of Fracture Mechanics to Crack Growth at Notches

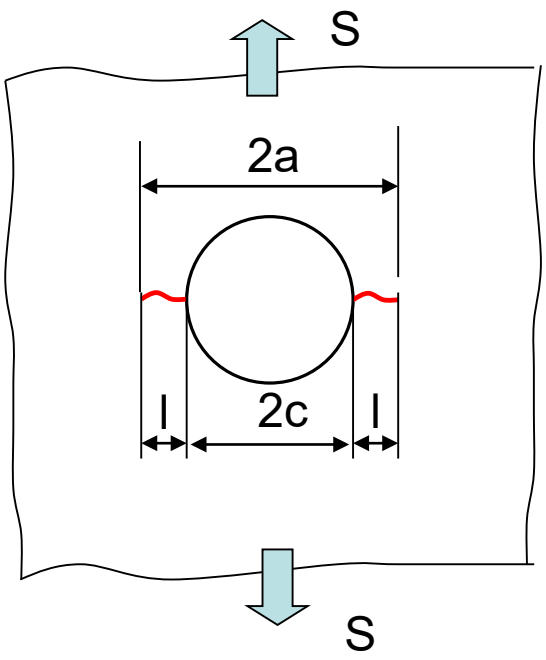

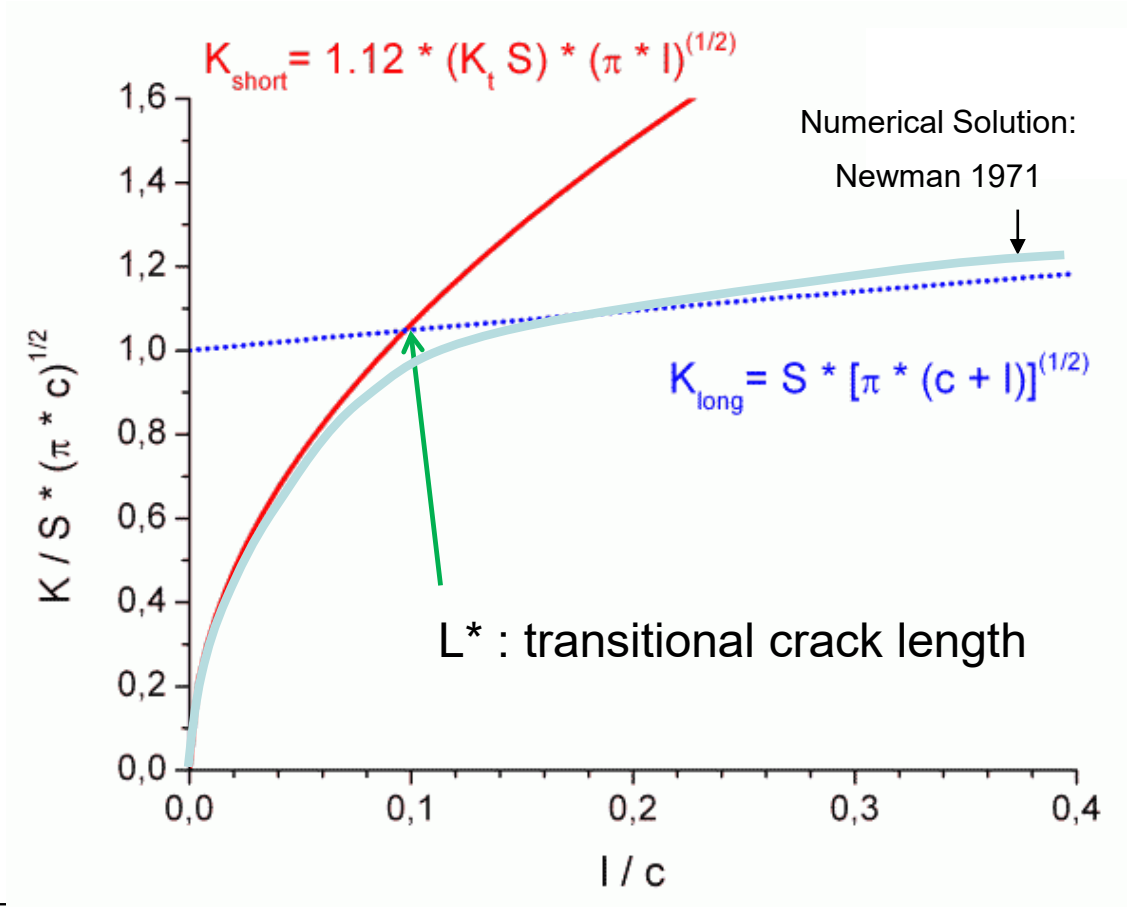

$$L^* = \frac{c}{(1.12 * K_t)^2 - 1}$$

Example:

2c = 5 mm, L* = 0.25 mm
2c = 25 mm, L* = 1.21 mm

For crack length l ≥ 10% c: **crack effective length is from tip to tip!!! (including notch)**

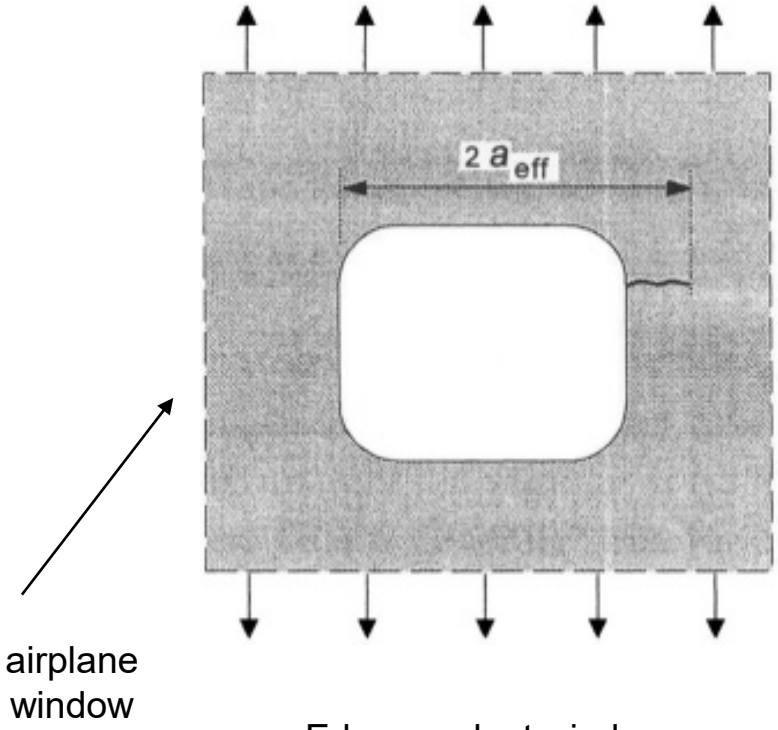

Edge crack at window

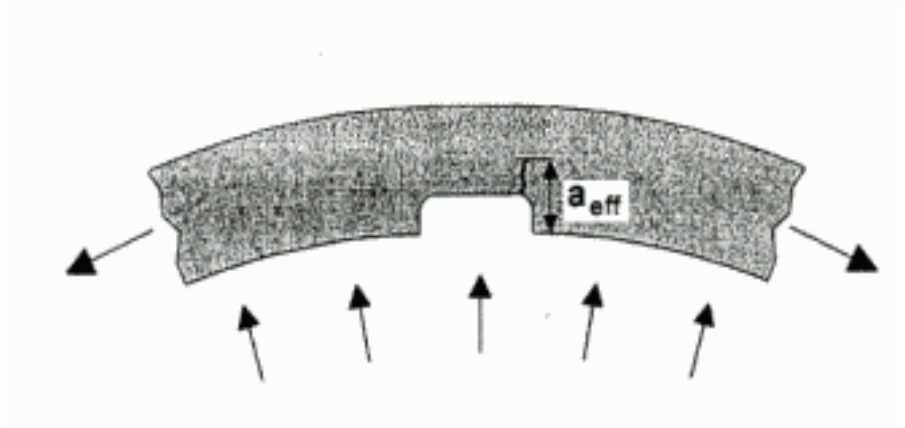

Crack in groove of a pressurized cylinder

Lager effective crack length by a contribution of a notch !

For relatively small (5-10 % notch size) cracks at a hole or at a notch, the stress intensity factor K is approximately the same as for a much larger crack with a length that includes the hole diameter / notch depth.

Reading: Fatige and the Comet Airplane (taken from S. Suresh, Fatigue of Materials)

Fatigue Crack Propagation

$\Delta K_{max} = K_{IC} (1-R)$!!

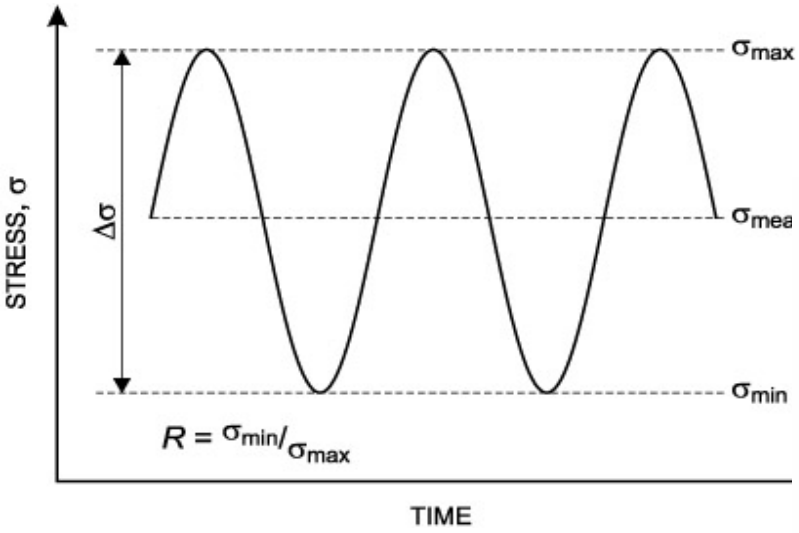

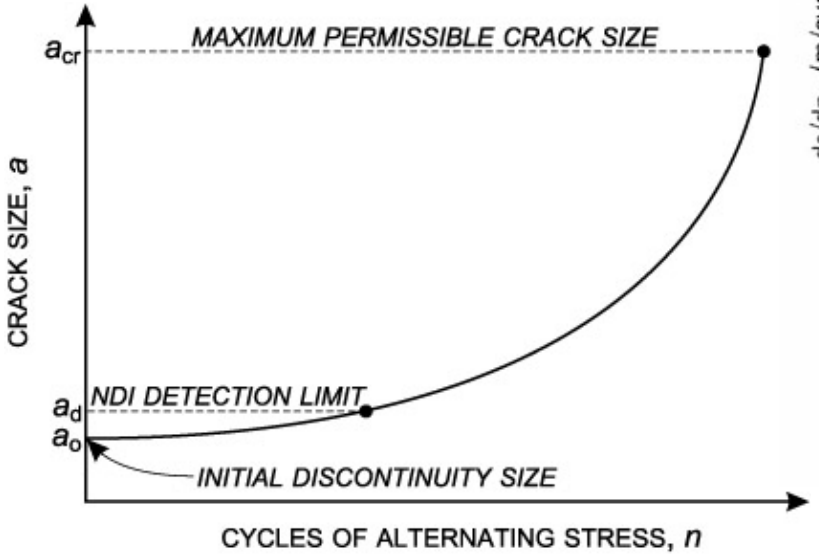

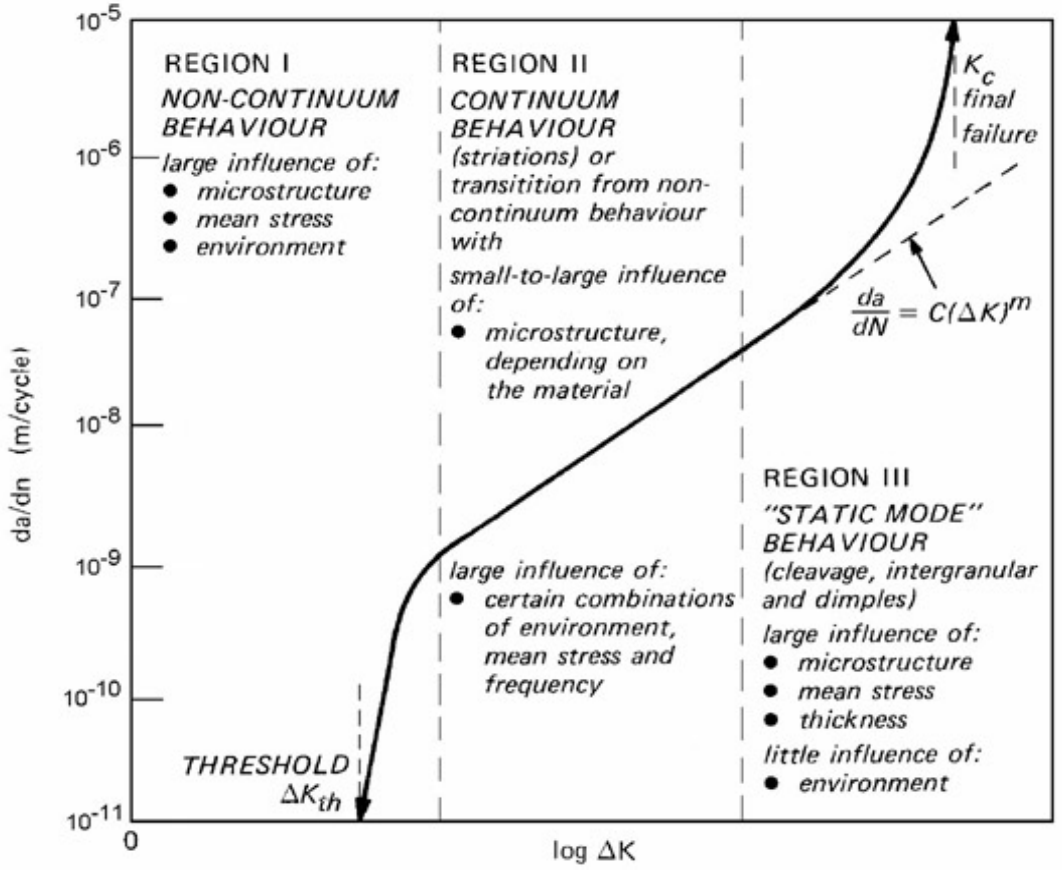

Fatigue crack growth rate curve da/dN - ΔK

How to describe crack growth rate curves: crack growth "laws"

Paris Law:

$$\frac{da}{dN} = C(\Delta K)^m$$

only Region II, no R effects

Forman:

$$\frac{da}{dN} = \frac{C(\Delta K)^m}{(1-R)K_{IC} - \Delta K}$$

also Region III

Complete curve

$$\frac{da}{dN} = C(\Delta K)^m \left\{ \frac{1 - \left(\frac{\Delta K_{th}}{\Delta K} \right)^{n_1}}{1 - \left(\frac{K_{\max}}{K_{IC}} \right)^{n_2}} \right\}^{n_3}$$

complete crack growth rate curve

n1, n2, n3, empirically adjusted parameters

McEvily:

$$\frac{da}{dN} = C(\Delta K - \Delta K_{th})^2 \left(1 + \frac{\Delta K}{K_{IC} - K_{\max}} \right)$$

the three regions

“Safe-life” vs “fail-safe” principle

- Another significant change and improvement in engineering practice: From 'safe-life' principle (establish life of a component without crack) to 'fail-safe' principle to establish period of crack growth from initial to critical value.
- Components are designed so that even if a crack exists with size below NDT threshold, it will not grow up to the critical size before the next examination, i.e. in the period between two NDT.

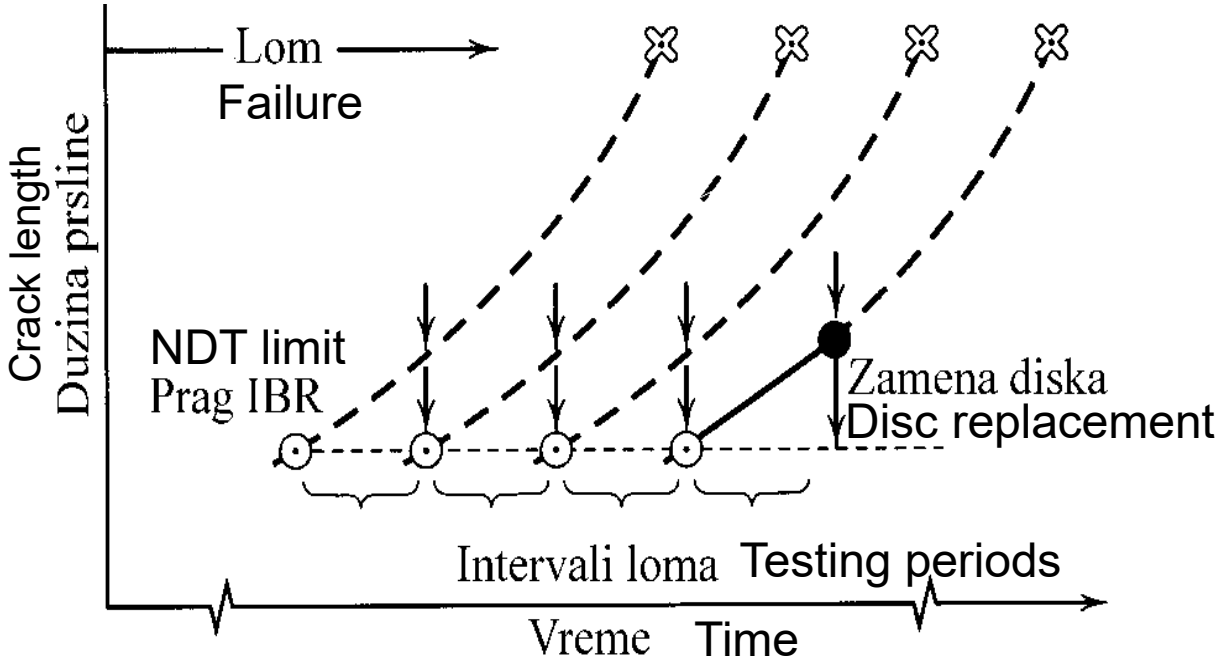

Paris Model for Fatigue Crack Growth Rate :

For design against fatigue failure, fracture mechanics is used to monitor the fatigue crack growth rate in the (stage II) Paris regime.

$$\frac{da}{dN} = A(\Delta K)^m$$

where the fatigue crack growth rate da/dN varies with stress intensity factor range ΔK, which is function of stress range Δσ and crack length *a*:

$$\Delta K = K_{\max} - K_{\min}$$

$$\Delta K = \sigma_{\max}\sqrt{\pi a} - \sigma_{\min}\sqrt{\pi a}$$

So the number of cycles for crack to grow from the initial to the critical value can be express as an integral:

$$N_f = \int_{a_0}^{a_c} \frac{da}{A\left(Y\Delta\sigma\sqrt{\pi a}\right)^m} = \frac{1}{A\pi^{m/2}(\Delta\sigma)^m}\int \frac{da}{Y^m a^{m/2}}$$

Experimental procedure for fatigue crack growth

- The fatigue crack growth rate, da/dN and stress intensity factor range at the fatigue threshold, ΔK_{th}, are experimentally tested.
- ASTM Standard E647, [28], provides procedures for fatigue crack growth rate, da/dN, testing and measurement and calculation of stress intensity factor range, ΔK. Standard Charpy specimens with fatigue crack in the base material (2 mm long) and with the foil RUMUL RMF A-5 for the continuous monitoring of crack length are used.
- Tests were conducted at room temperature with three-point bending in load control, and a high-frequency resonant pulsator Cracktronic is used.

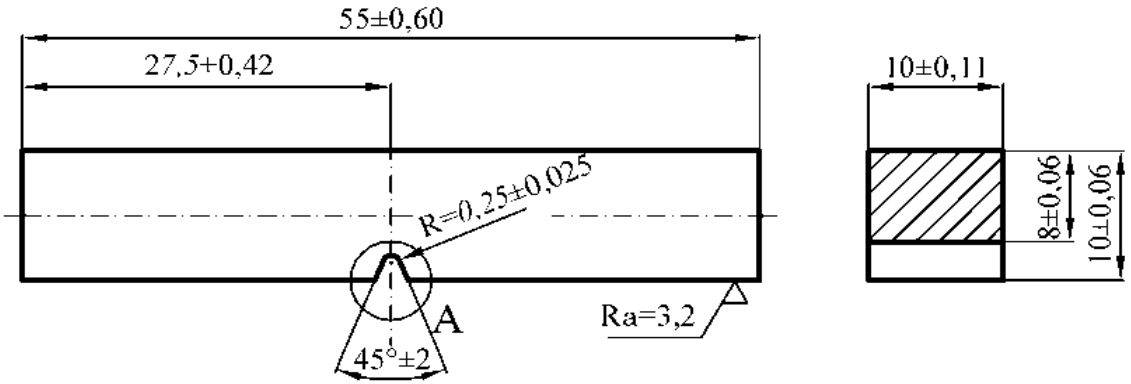

Integrity and life assessment of Ti-6Al-4V Total Hip implant

- The function of Total Hip Replacement is to carry the load induced by normal everyday activity.
- Loads that occur on Total Hip Replacement implants can be as high as 8.7 times the body weight of a patient.
- Total Hip Replacement failure may be caused by implant loosening, wear of material, or fatigue (which is the most common cause).
- In combination with defects, such as inclusions and micro cracks in Total Hip Replacement implants, fatigue crack initiation is the most probable at locations of maximal stress state, i.e. stress concentration regions.

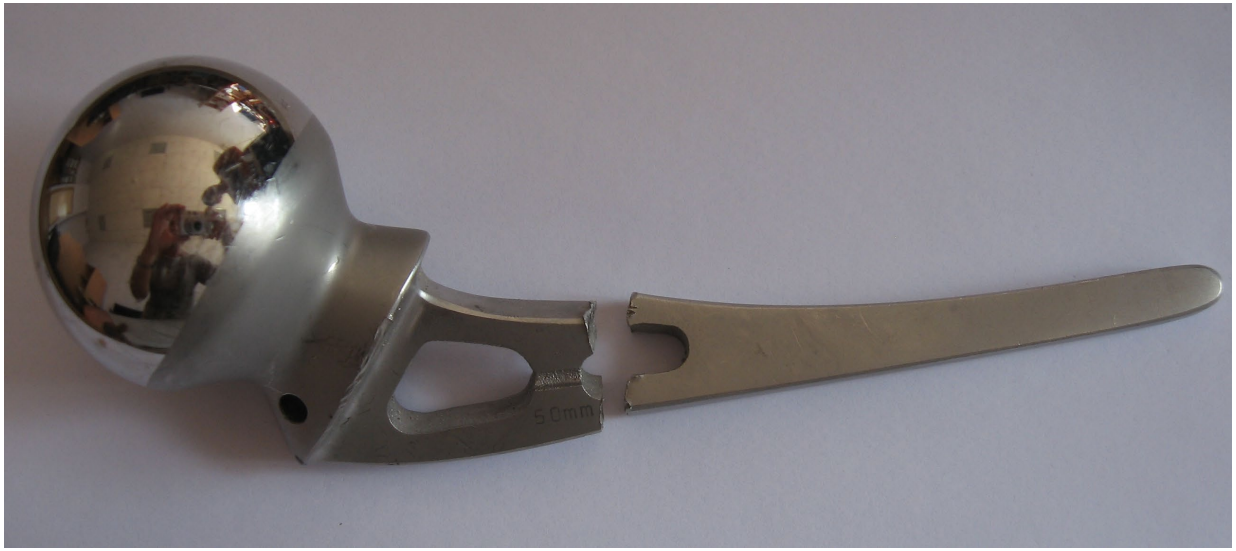

Static model in ABAQUS

- After the CAD model was verified, a STEP file was made, and imported into ABAQUS, for stress analysis.
- This was done in order to determine critical locations in terms of stress concentration.
- In the next stage, a crack was defined at the location of highest stress concentration

Mechanical properties for LE analysis

Material	Young's modulus (GPa)	Poisson coefficient
Ti6Al4V ELI	120	0.3
Zirconia Y-TZP	205	0.3

Static model in ABAQUS

- Boundary conditions were defined by fixing the implant surfaces in contact with the femur bone.
- The load was defined as a concentrated force, acting on the implant head, via reference point. Its magnitude was 7681 N.

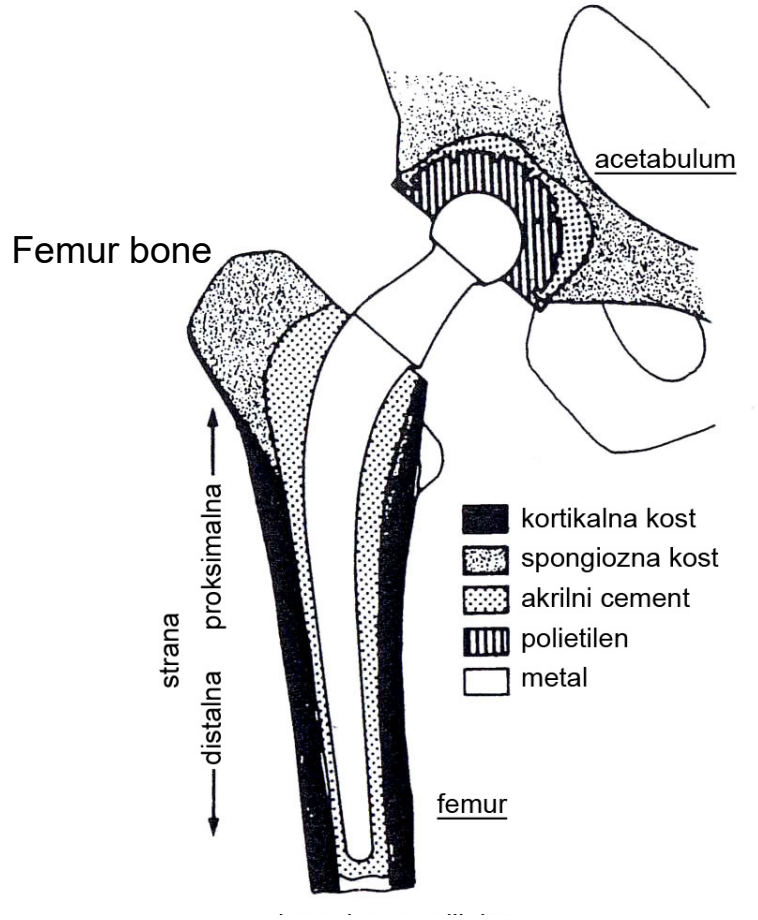

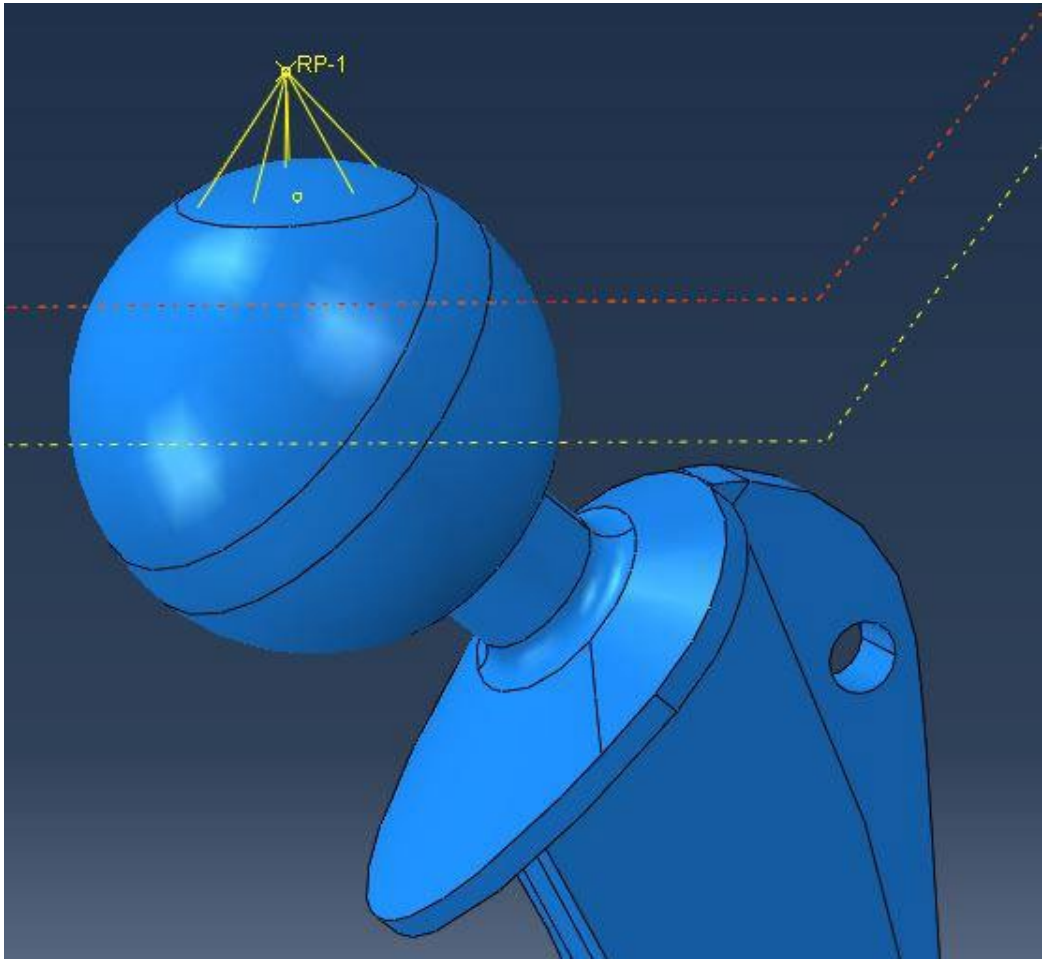

Static model in ABAQUS

- The stress concentration area is mostly pronounced wider at the back side of the implant neck. This indicates a potential location for crack initiation.
- Stresses were significantly below yield values, hence only linear elastic analysis was carried out in this stage.

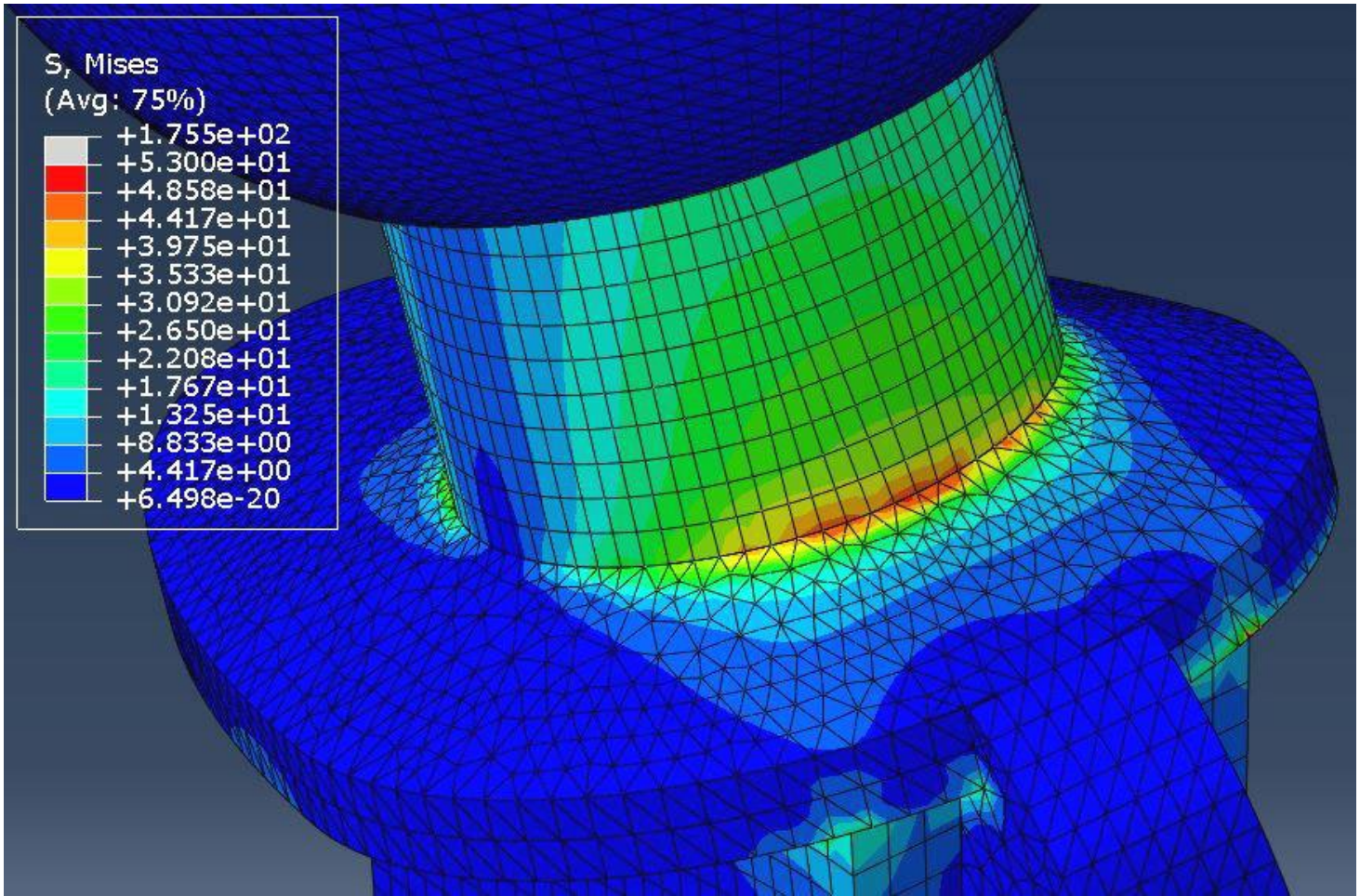

Fatigue crack growth

- Fatigue crack growth simulation was performed in ANSYS R19.2.
- Initial crack depth was 1 mm, since this is the minimum crack length that can be detected using NDT methods.
- The model was meshed using TET elements, due to software requirements.
- The load was defined in the same way as in the static case, directly on the top surface of the head, and the boundary fixed support BC defined on the stem.

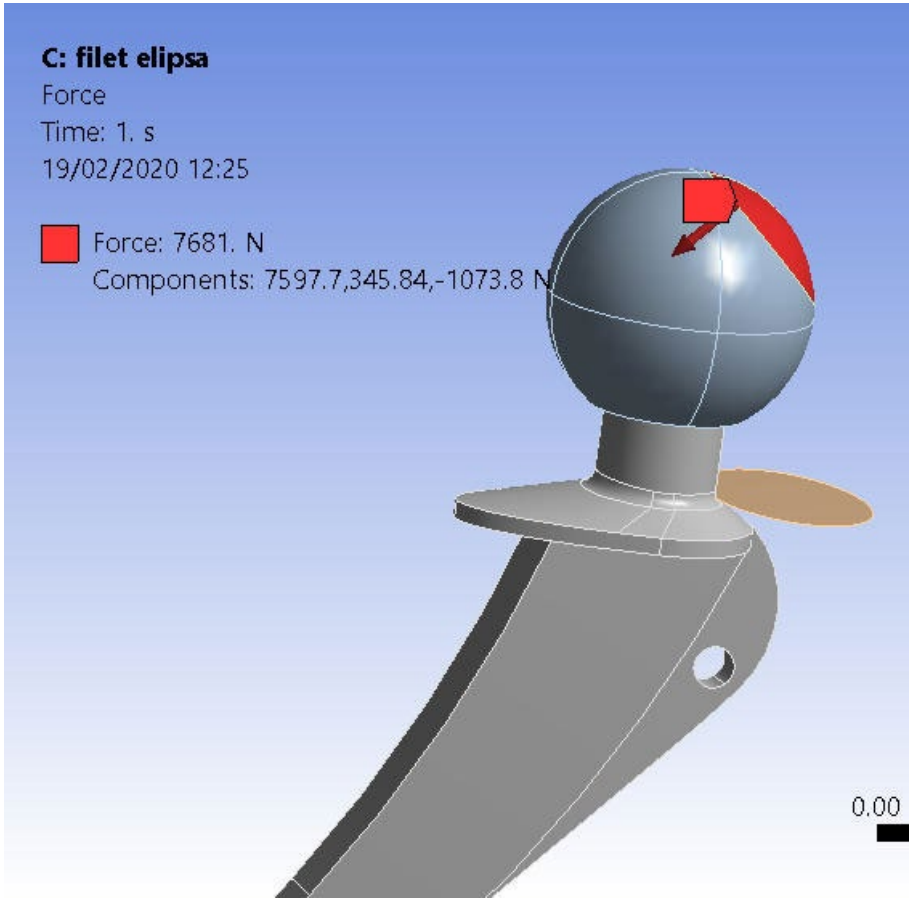

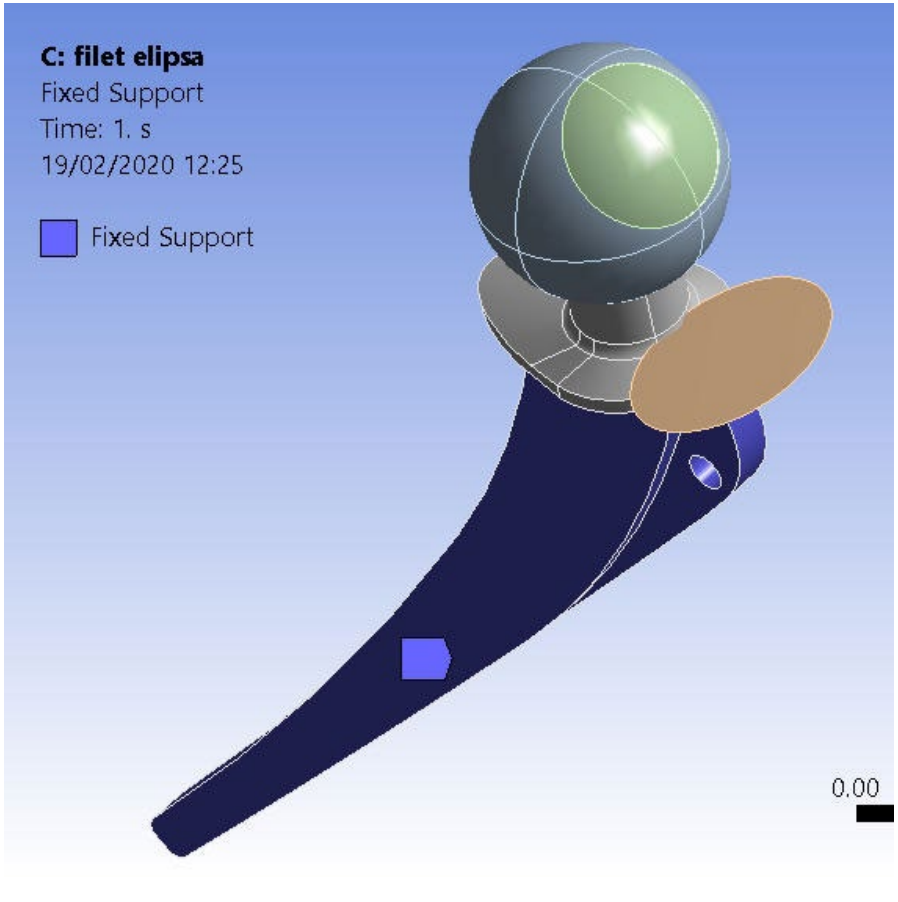

Fatigue crack growth - results

- Deformed model, with total deformation distribution in mm

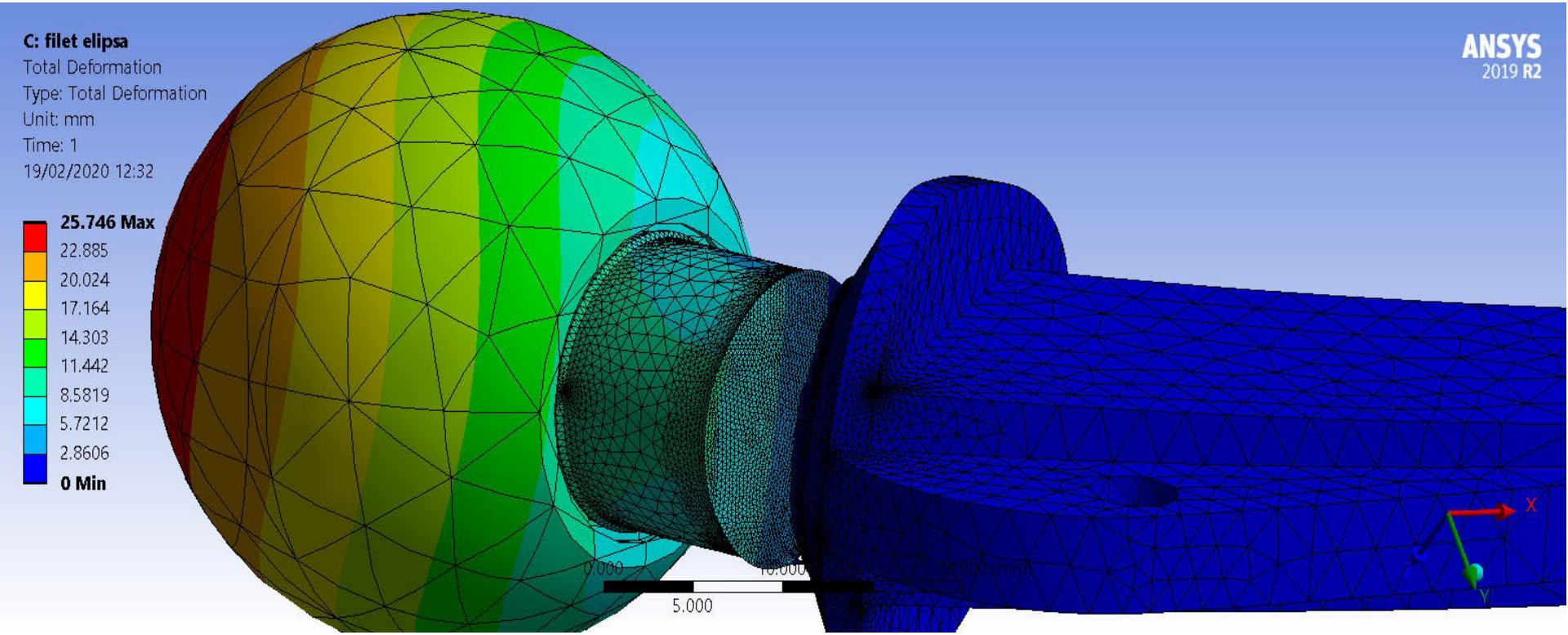

Fatigue crack growth

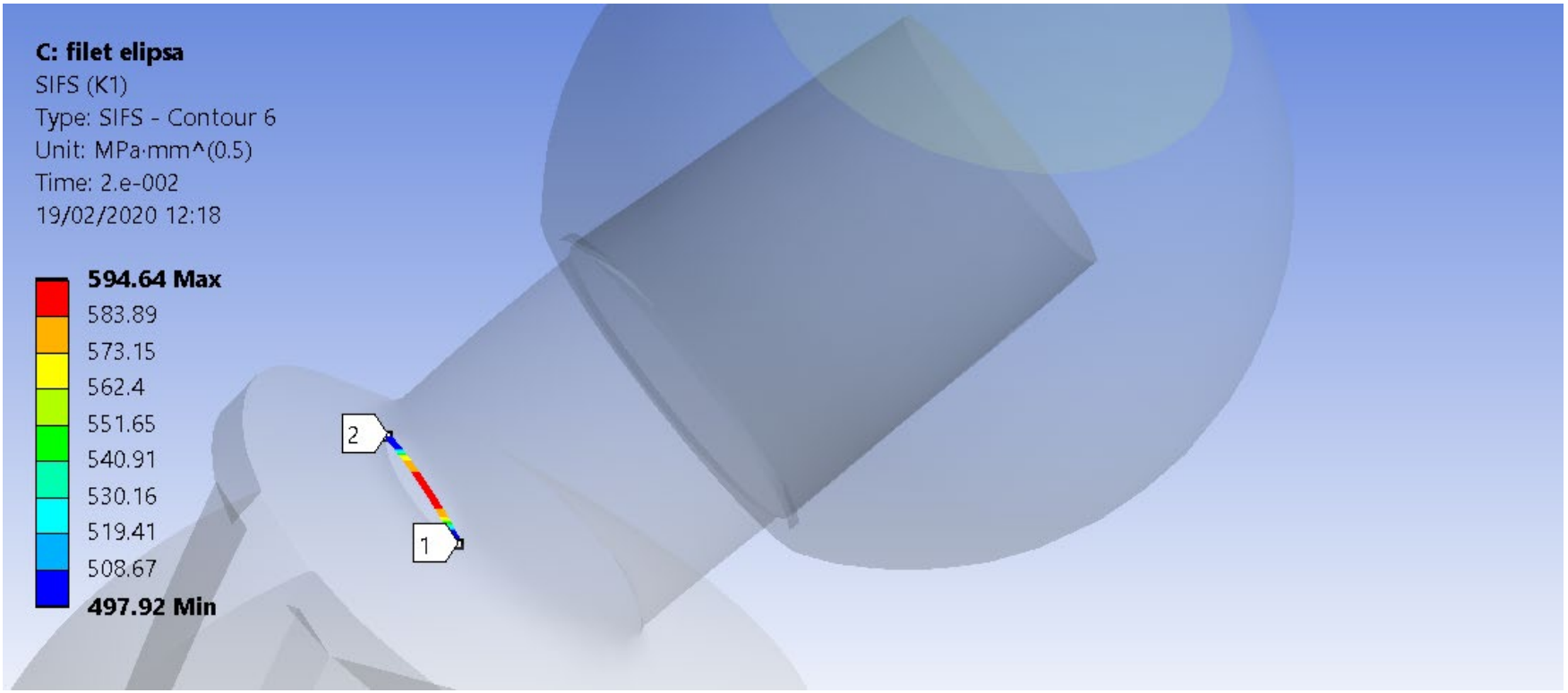

- Stress Intensity Factors (SIF)

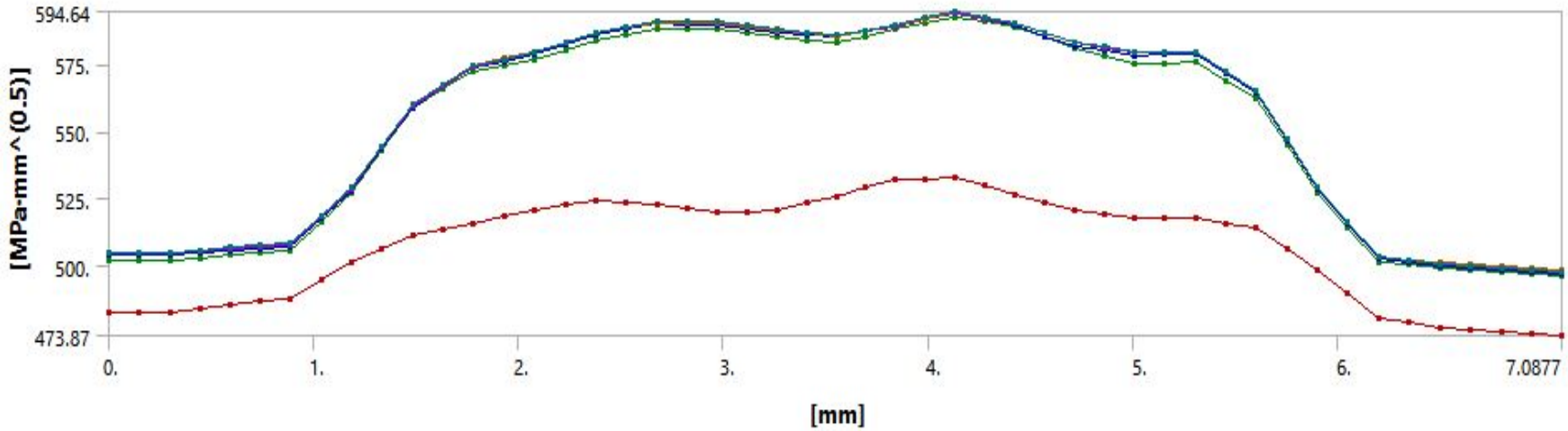

Fatigue crack growth - results

- Crack length vs number of cycles curve (a-N)

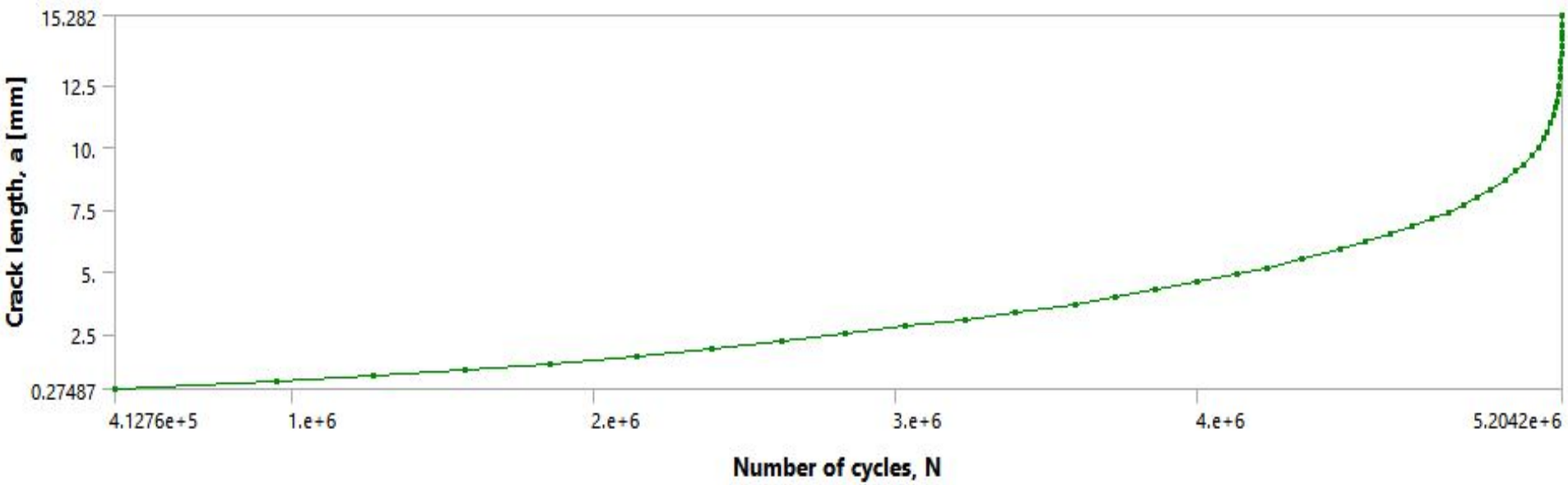

- Total number of cycles was 5,204,200.
- This amount is of the same order of magnitude as in other, similar models/experiments.
- Hence, the model provided solid results, even without its own experiment.
- Closed circle of 3D scanning, CAD modelling, numerical simulation (i.e. Finite Element Analysis) and manufacturing using newly developed additive technologies will present a new trend in implant manufacture.
- This approach provided satisfying results, which will be used as a base for further research. This research will involve different hip geometries and different materials.